# Remote Sensing of Tree Growth - New Approaches for Monitoring Annual Growth Onset and Intra-annual Variability

A Thesis

Presented in Partial Fulfillment of the Requirements

for the

Degree of Master of Science

with a

Major in Natural Resources

in the

College of Graduate Studies

University of Idaho

by

William A. Weygint

Approved by:

Major Professor: Jan Eitel, Ph.D.

Committee Members: Lee Vierling, Ph.D.; Colin Campbell, Ph.D.;

Daniel Johnson, Ph.D.

Department Administrator: Kerri Vierling, Ph.D.

May 2022

# Abstract

Tree growth is mechanistically linked to the global water and carbon (C) cycles and is thus a key area of research. As part of this research studies have explored linkages between remote sensing data products and tree growth, but the majority of this research has focused on tracking photosynthesis and *inter*-annual tree growth. Only a fewstudies have explored *intra*-annual stem radial growth, which provides information on long term carbon sequestration.

The following chapters explore new remote sensing-based approaches for monitor intra-annual stem radial growth in North American forests. Chapter 1 outlines some of the previous work that has used remote sensing approaches to monitor tree growth, as well as some of the potential challenges that exist.

Chapter 2 explores possible connections between remotely sensed snow disappearance date and the onset of stem radial growth in conifers at the forest-tundra ecotone (FTE) in North America. Specifically, we posed two hyphotheses: 1) that satellite based SDD estimates from the Moderate Resolution Imaging Spectroradiometer ($SDD_{MODIS}$) are not significantly ($p < 0.05$) different than *in situ* measurements of SDD from soil temperature probes ($SDD_{ST}$), thereby suggesting that $SDD_{MODIS}$ is a reliable proxy for *in situ* SDD, and; 2) that estimates of SDD are not significantly different than the onset of tree radial growth, implying that $SDD_{MODIS}$ could reliably detect the start of tree wood growth at the FTE. To test our hypotheses, we used data from two field sites at the FTE - one located in Alaska (AK) and one in the Northwest Territory (NWT). $SDD_{MODIS}$ and $SDD_{ST}$ were synchronous at AK, while they were asynchronous at NWT. Both SDD estimates were significantly different from tree growth onset at AK in both years but were similar in NWT. These results highlight the ecological heterogeneity of the FTE and the key knowledge gaps remaining in our understanding of environmental factors driving tree growth at this ecotone. However, our finding that remote estimates of SDD were statistically similar to tree growth onset at one field site demonstrates that remote sensing holds promise for detecting shifts in springtime tree growth phenology in response to climate change at the FTE.

Chapter 3 explores connections between branch level remotely sensed leaf

temperatures ($T_L$) and intra-annual stem radial variations (SRVs). We posed two main questions. Can we use a combination of remote sensing information and environmental variables to predict 1) tree water status, and 2) tree growth? Within Question 2, we also had two sub-questions: 2.1) Can we predict if trees are growing or not, and 2.2) Based on the results of Question 2.1, can we predict the amount of daily growth? We hypothesized that the strength of the relationship between remotely sensed $T_L$ and SRVs would vary depending on the time of day which $T_L$ was measured. We used an existing environmental monitoring network that collected near continuous SRV and $T_L$ measurements through the 2019 – 2021 growing seasons to answer these questions. Results showed that $T_L$, along with other environmental variables, could predict SRVs reasonably well, with maximum $R^2$ values between 0.5 – 0.75 for the best models. However, the time of day which $T_L$ was measured also changed the strength of the models, as well as the shape of the predicted model curves. These results show promise for using remotely sensed $T_L$ as a proxy for daily SRVs, though there are still key questions that remain, including how well the observed relationships scale to coarser spatial scales. This project provides a crucial first step in the development of novel remote sensing based approaches for monitoring intra-annual SRVs and outlines potential future directions.

Chapter 4 highlights some of the key findings from Chapters 2 and 3, and discusses potential avenues for future research. One highlighted area of future research includes scaling stem radial growth measurements up to a spatial and temporal resolutions equivalent to many airborne and satellite remote sensing data products. This will be a crucial area of research to continue evaluating how well remote sensing products can monitor stem radial growth in North American forests.

# Acknowledgments

I would like to acknowledge the support of my advisor, Jan Eitel, as well as the other members of my committee (Lee Vierling, Colin Campbell, and Daniel Johnson) for helping guide me through this process. I would also like to thank current and former lab members, including Andrew Maguire, Jyoti Jennewein, and Eli Estey for their friendship and support. Finally, I would like to acknowledge funding support from NASA under grant #80NSSC20M108. The funders had no role in study design, data collection and analysis, decision to publish, or preparation of the manuscript (thesis).

## Dedication

I would like to thank my family for their support during this process. I would also like to thank those in the University of Idaho community, both in Moscow and McCall, who have supported me and who I have learned immensely from. You have made me feel that I am part of a community for which I am tremendously grateful.

# Table of Contents

# List of Tables

# List of Figures

## Statement of Contribution

The chapters of this thesis are primarily authored by William A. Weygint. Weygint was the leader during project development, analysis, and writing on all following chapters. Co-authors for Chapter 2 include Jan U.H. Eitel, Andrew J. Maguire, Lee A. Vierling, Kevin L. Griffin, Natalie T. Boelman, and Johanna E. Jensen. Co-authors for Chapter 3 include Jan U.H. Eitel, Lee A. Vierling, Andrew J. Maguire, Daniel M. Johnson, Colin S. Campbell, and Kevin L. Griffin. For both chapters co-authors assisted in data collection, provided feedback on analysis, and assisted in revising the final manuscript.

# Chapter 1: Introduction

Forests occupy roughly half of the Earth's land surface (Boisvenue and Running, 2006) and make important contributions to global water and carbon cycles, contributing to over 40% of the terrestrial carbon sink (Le Quéré et al., 2012; Pan et al., 2011). Besides their importance as a global carbon (C) sink, forests provide other benefits, including serving as habitat for a variety of animals and plants. Forests also serve as homes for 1.6 billion people across the world, including 11% of the population of the United States (Newton et al., 2020), and provide ecosystem services (e.g., timber production, freshwater reservoirs, etc.) which people worldwide depend on. Given the socioecological importance of forests it is critical that robust, effective monitoring systems are in place to detect changes in forest structure and function, as well as determine how these changes may impact ecosystem services which human communities rely on.

Human-induced climate change is affecting boreal and temperate forests across North America in numerous ways but is having particularly detrimental impacts to hydrologic regimes (Fyfe et al., 2017; Mote et al., 2018). Both forest types are located mostly in high-latitude or high-elevation regions and as such are characterized by long, cold winters with a seasonal snowpack and short growing seasons. There is evidence that seasonal snowpacks influence numerous forest processes, including the onset of the growing season and water availability for tree growth (Rossi et al., 2011; Vaganov et al., 1999). Thus, any changes in the amount and duration of seasonal snowpacks in North American forests could affect physiological processes that influence important ecosystem services.

Climate-change induced effects on seasonal snowpacks in North America are already being observed, including declines in the amount of snow each winter as well as changes in the length of the snow season, typically in the form of earlier snow melt (Fyfe et al., 2017; Mote et al., 2018). While some studies have explored the effects of these changing snow regimes on tree growth (Bowling et al., 2018; Rasmus et al., 2011), more

robust methods are needed to assess the impacts of these alterations on subsequent tree growth.

Stem radial growth is a foundational physiological process with key linkages to global C and water cycles (Drew and Downes, 2009). Thus, this process is uniquely suited to provide information on hydrologic-related changes to tree growth in forested ecosystems. Stem radial growth is the expansion of a tree bole over time, and this expansion can be measured at diurnal and seasonal (*intra*-annual growth), or yearly (*inter*-annual growth) time scales (De Swaef et al., 2015; Drew and Downes, 2009). Radial growth occurs when there is sufficient water in the cambial cells to increase the turgor potential enough to allow cell expansion and division (Jones, 2014). During wood production C is then captured and stored in the new wood for decades to centuries. While many studies have used inter-annual growth measurements to determine the efficiency of carbon uptake for a given growing season, intra-annual tree growth may be better suited to study carbon uptake efficiency and how it responds to within-season variability in growth conditions.

Intra-annual stem radial growth can be measured in-situ using point dendrometers, which are instruments that are fixed to a tree bole and can detect micrometer level expansions and contractions of stem radius (referred to as stem radial variations, or SRVs) at very high temporal resolutions (minutes to hours) (Drew and Downes, 2009). SRVs have been used to monitor tree water status, stem radial growth and the onset of radial growth in forests (Dietrich et al., 2018; Eitel et al., 2020; Oberhuber, 2017; Zweifel et al., 2021, 2005). While dendrometers provide a wealth of ecophysiological information, they do have their limitations, mainly that they can only provide spatially limited information and that large dendrometer networks are expensive and time consuming to install and maintain. Thus, it can be difficult to generalize the results from these fine-scale physiological measurements across entire forested ecosystems. Developing approaches to assess these intra-annual SRVs across entire ecosystems and regions is vital to allow an understanding of sub-yearly changes in forest hydrologic and C regimes.

Remote sensing techniques are also well positioned to monitor climate-induced alterations to tree growth. From the advent of Earth-orbiting satellites like Landsat, remote sensing technologies have been able to measure processes related to forest function and change (Dye and Tucker, 2003; Loveland and Dwyer, 2012; Tucker and Sellers, 1986). To do so a wide range of remote sensing data products have been developed, which provide information on many inter-annual tree growth processes, including vegetative phenology (Dye and Tucker, 2003; Karkauskaite et al., 2017; Karlsen et al., 2008), plant growth (Berner et al., 2013; White et al., 2016), and C cycling and sequestration (Xiao et al., 2004; Zhu et al., 2016). Many of these products are also easy to obtain and use compared to traditional forest mensuration approaches which often require costly field sampling to collect spatially limited data (Kerr and Ostrovsky, 2003; Marceau and Hay, 1999). These technologies allowed researchers and managers to conduct ecosystem level studies that were not possible solely with in-situ methods, getting looks at how water availability, C cycling, and plant growth varied across entire landscapes (Kerr and Ostrovsky, 2003). However, few remote sensing approaches for tracking intra-annual tree growth have been developed, which leaves a critical knowledge gap in our understanding of how carbon, water, and other key nutrient cycles that are closely linked to tree growth vary across regions and ecosystems.

Linking point dendrometer measurements with remote sensing methods could provide a robust technique for monitoring intra-annual stem radial growth at ecosystem scales and how this process will respond to climate change. However, before airborne and spaceborne level remote sensing data can be used, relationships must be studied between SRVs and in-situ sensors acquiring branch or tree level remote sensing data. This is a crucial step for any remote sensing technique as field studies help to identify linkages between remotely sensed information and the physiological process of interest (e.g., tree growth) that might be more difficult to identifyfrom airborne or satellite remote sensing data (Zellweger et al., 2019). Field studies can also highlight potential challenges to using satellite level data as well. An example of a study that used in-situ remote sensing information is Eitel et al. (2020), who explored if a remotely sensed vegetation index (e.g., photochemical reflectance index, or PRI) could track intra-annual radial growth in conifers at eh forest-tundra ecotone. They used branch level PRI data to answer

this question and found that PRI closely tracked stem radial growth through the growing season and highlighted some of the challenges that could be associated with using coarser scale PRI data (e.g., variation in background reflectance, cloud and snow cover, and the scalability of the observed mechanistic relationships between PRI and growth) for monitoring stem radial growth (Eitel et al., 2020). Thus, this study demonstrates the tremendous value of in-situ remote sensing studies to develop and validate remote sensing approaches for monitoring physiological processes at the landscape scale.

The following chapters explore relationships between various remote sensing techniques and stem radial growth metrics to better understand if remote sensing approaches can be used to track intra-annual stem radial growth in North American forests. Chapter 2 evaluates the effectiveness of using remotely sensed snow disappearance date (SDD) estimates for detecting the onset of stem radial growth in conifers at the FTE. Past studies have shown that SDD and radial growth onset correspond well in high latitude forests (Rossi et al., 2011; Vaganov et al., 1999), while other remote sensing indices have had success in predicting the end of the growing season at the FTE (Eitel et al., 2020). Thus, SDD (if shown to be effective) combined with other remote sensing information, could provide an accurate estimate of the length of the growing season in high-latitude forests.

Chapter 3 explores connections between branch level remotely sensed $T_L$ and SRVs in a subalpine temperate forest. Due to the mechanistic linkages to tree water status, $T_L$ is well positioned to detect and monitor intra-annual changes in SRVs. This work lays the foundation for future work exploring the suitability of using $T_L$ as a proxy for SRVs in temperate coniferous forests and is made relevant by the recent (as of 2022) launch of several spaceborne instruments (e.g., ECOSTRESS and Landsat 9) which measure $T_L$ at increasing spatial and temporal resolutions. Chapter 4 highlights the key findings of chapter 2 and 3 and outlines potential future research areas to continue developing the remote sensing approaches described in chapters 2 and 3.

***References***

Berner, L.T., Beck, P.S.A., Bunn, A.G., Goetz, S.J., 2013. Plant response to climate change along the forest-tundra ecotone in northeastern Siberia. Glob. Chang. Biol. 19, 3449–3462. https://doi.org/10.1111/gcb.12304

Boisvenue, C., Running, S.W., 2006. Impacts of climate change on natural forest productivity - Evidence since the middle of the 20th century. Glob. Chang. Biol. 12, 862–882. https://doi.org/10.1111/j.1365-2486.2006.01134.x

Bowling, D.R., Logan, B.A., Hufkens, K., Aubrecht, D.M., Richardson, A.D., Burns, S.P., Anderegg, W.R.L., Blanken, P.D., Eiriksson, D.P., 2018. Limitations to winter and spring photosynthesis of a Rocky Mountain subalpine forest. Agric. For. Meteorol. 252, 241–255. https://doi.org/10.1016/j.agrformet.2018.01.025

De Swaef, T., De Schepper, V., Vandegehuchte, M.W., Steppe, K., 2015. Stem diameter variations as a versatile research tool in ecophysiology. Tree Physiol. https://doi.org/10.1093/treephys/tpv080

Dietrich, L., Zweifel, R., Kahmen, A., 2018. Daily stem diameter variations can predict the canopy water status of mature temperate trees. Tree Physiol. 38, 941–952. https://doi.org/10.1093/treephys/tpy023

Drew, D.M., Downes, G.M., 2009. The use of precision dendrometers in research on daily stem size and wood property variation: a review. Dendrochronologia 27, 159–172.

Dye, D.G., Tucker, C.J., 2003. Seasonality and trends of snow-cover, vegetation index, and temperature in northern Eurasia. Geophys. Res. Lett. 30, 3–6. https://doi.org/10.1029/2002GL016384

Eitel, J.U.H., Griffin, K.L., Boelman, N.T., Maguire, A.J., Meddens, A.J.H., Jensen, J., Vierling, L.A., Schmiege, S.C., Jennewein, J.S., 2020. Remote sensing tracks daily radial wood growth of evergreen needleleaf trees. Glob. Chang. Biol. 1–11. https://doi.org/10.1111/gcb.15112

Fyfe, J.C., Derksen, C., Mudryk, L., Flato, G.M., Santer, B.D., Swart, N.C., Molotch, N.P., Zhang, X., Wan, H., Arora, V.K., Scinocca, J., Jiao, Y., 2017. Large near-Term projected snowpack loss over the western United States. Nat. Commun. 8, 1–7. https://doi.org/10.1038/ncomms14996

Jones, H.G., 2014. Plants and Microclimate: A Quantitative Approach to Environmental Plant Physiology, 3rd ed. Cambridge University Press.

Karkauskaite, P., Tagesson, T., Fensholt, R., 2017. Evaluation of the Plant Phenology Index (PPI), NDVI and EVI for Start-of-Season Trend Analysis of the Northern Hemisphere Boreal Zone. Remote Sens. 9, 485. https://doi.org/10.3390/rs9050485

Karlsen, S.R., Tolvanen, A., Kubin, E., Poikolainen, J., Arild, K., Johansen, B., Danks, F.S., Aspholm, P., Emil, F., Makarova, O., 2008. MODIS-NDVI-based mapping of the length of the growing season in northern Fennoscandia. Int. J. Appl. Earth Obs. Geoinf. 10, 253–266. https://doi.org/10.1016/j.jag.2007.10.005

Kerr, J.T., Ostrovsky, M., 2003. From space to species: Ecological applications for remote sensing. Trends Ecol. Evol. 18, 299–305. https://doi.org/10.1016/S0169-5347(03)00071-5

Le Quere, C., Andres, R.J., Boden, T., Conway, T., Houghton, R.A., House, J.I., Marland, G., Peters, G.P., van der Werf, G., Ahlstrom, A., Andrew, R.M., Bopp, L., Canadell, J.G., Ciais, P., Doney, S.C., Enright, C., Friedlingstein, P., Huntingford, C., Jain, A.K., Jourdain, C., Kato, E., Keeling, R.F., Goldewijk, K.K., Levis, S., Levy, P., Lomas, M., Poulter, B., Raupach, M.R., Schwinger, J., Sitch, S., Stocker, B.D., Viovy, N., Zaehle, S., Zeng, N., 2012. The global carbon budget 1959–2011. Earth Syst. Sci. Data Discuss. 5, 1107–1157. https://doi.org/10.5194/essdd-5-1107-2012

Loveland, T.R., Dwyer, J.L., 2012. Landsat: Building a strong future. Remote Sens. Environ. 122, 22–29. https://doi.org/10.1016/j.rse.2011.09.022

Marceau, D.J., Hay, G.J., 1999. Remote sensing contributions to the scale issue. Can. J. Remote Sens. 25, 357–366. https://doi.org/10.1080/07038992.1999.10874735

Mote, P.W., Li, S., Lettenmaier, D.P., Xiao, M., Engel, R., 2018. Dramatic declines in snowpack in the western US. npj Clim. Atmos. Sci. https://doi.org/10.1038/s41612-018-0012-1

Newton, P., Kinzer, A.T., Miller, D.C., Oldekop, J.A., Agrawal, A., 2020. The Number and Spatial Distribution of Forest-Proximate People Globally. One Earth 3, 363–370. https://doi.org/10.1016/j.oneear.2020.08.016

Oberhuber, W., 2017. Soil water availability and evaporative demand affect seasonal growth dynamics and use of stored water in co-occurring saplings and mature conifers under drought. Trees - Struct. Funct. 31. https://doi.org/10.1007/s00468-016-1468-4

Pan, Y., Birdsey, R.A., Fang, J., Houghton, R., Kauppi, P.E., Kurz, W.A., Phillips, O.L., Shvidenko, A., Lewis, S.L., Canadell, J.G., Ciais, P., Jackson, R.B., Pacala, S.W., McGuire, A.D., Piao, S., Rautianeri, A., Sitch, S., Hayes, D., 2011. A large and persistent carbon sink in the world's forests. Science (80-. ). 333, 988–993.

Rasmus, S., Lundell, R., Saarinen, T., 2011. Interactions between snow, canopy, and vegetation in a boreal coniferous forest. Plant Ecol. Divers. 4, 55–65. https://doi.org/10.1080/17550874.2011.558126

Rossi, S., Morin, H., Deslauriers, A., 2011. Multi-scale influence of snowmelt on xylogenesis of black spruce. Arctic, Antarct. Alp. Res. 43, 457–464. https://doi.org/10.1657/1938-4246-43.3.457

Tucker, C.J., Sellers, P.J., 1986. Satellite remote sensing of primary production. Int. J. Remote Sens. 7, 1395–1416. https://doi.org/10.1080/01431168608948944

Vaganov, E.A., Hughes, M.K., Kirdyanov, A. V, Schweingruber, F.H., Silkin, P.P., 1999. Influence of snowfall and melt timing on tree growth in subarctic Eurasia. Nature 400, 149–151.

White, J.C., Coops, N.C., Wulder, M.A., Vastaranta, M., Hilker, T., Tompalski, P., White, J.C., Coops, N.C., Wulder, M.A., Vastaranta, M., White, J.C., Coops, N.C., Wulder, M.A., Vastaranta, M., Hilker, T., Tompalski, P., 2016. Remote Sensing

Technologies for Enhancing Forest Inventories: A Review. Can. J. Remote Sens. 42, 619–641. https://doi.org/10.1080/07038992.2016.1207484

Xiao, X., Hollinger, D., Aber, J., Goltz, M., Davidson, E.A., Zhang, Q., Moore, B., 2004. Satellite-based modeling of gross primary production in an evergreen needleleaf forest. Remote Sens. Environ. 89, 519–534.

Zellweger, F., De Frenne, P., Lenoir, J., Rocchini, D., Coomes, D., 2019. Advances in Microclimate Ecology Arising from Remote Sensing. Trends Ecol. Evol. 34, 327–341. https://doi.org/10.1016/j.tree.2018.12.012

Zhu, Z., Piao, S., Myneni, R.B., Huang, M., Zeng, Z., Canadell, J.G., Ciais, P., Sitch, S., Friedlingstein, P., Arneth, A., Liu, R., Mao, J., Pan, Y., Peng, S., Peñuelas, J., Poulter, B., 2016. Greening of the Earth and its drivers. Nat. Clim. Chang. 6, 791–796. https://doi.org/10.1038/NCLIMATE3004

Zweifel, R., Sterck, F., Braun, S., Buchman, N., Eugster, W., Gessler, A., Hani, M., Peters, R.L., Walthert, L., Wilhelm, M., Zieminska, K., Etzold, S., 2021. Why trees grow at night. New Phytol. 1–29. https://doi.org/10.1111/nph.17552

Zweifel, R., Zimmermann, L., Newbery, D.M., 2005. Modeling tree water deficit from microclimate : an approach to quantifying drought stress. Tree Physiol. 25, 147–156.

# Chapter 2: Determining the Suitability of Remotely Sensed Snow Disappearance Date as a Proxy for the Onset of Tree Wood Growth in Conifers at the Forest Tundra Ecotone


## Abstract

Tree wood growth is a key phenological process governing the seasonal duration of carbon sequestration, but relatively little is known about how climate change affects tree growth. Hence, methods for detecting and monitoring tree growth onset are needed, particularly in regions like the forest-tundra ecotone (FTE) that are sensitive to climatic changes. Because snow disappearance date (SDD) is observable across large spatial scales using satellite remote sensing and may influence tree growth onset, we tested the reliability of remotely sensed SDD as a proxy for tree wood growth onset at the FTE. We pose two research hypotheses: 1) that satellite based SDD estimates from the Moderate Resolution Imaging Spectroradiometer ($SDD_{MODIS}$) are not significantly ($p < 0.05$) different than *in situ* measurements of SDD from soil temperature probes ($SDD_{ST}$), thereby suggesting that $SDD_{MODIS}$ is a reliable proxy for *in situ* SDD, and; 2) that estimates of SDD are not significantly different than the onset of tree radial growth, implying that $SDD_{MODIS}$ could reliably detect the start of tree wood growth at the FTE. To test our hypotheses, we used data from two field sites at the FTE - one located in Alaska (AK) and one in the Northwest Territory (NWT). $SDD_{MODIS}$ and $SDD_{ST}$ were synchronous at AK, while they were asynchronous at NWT. Both SDD estimates were significantly different from tree growth onset at AK in both years but were similar in NWT. These results highlight the ecological heterogeneity of the FTE and the key knowledge gaps remaining in our understanding of phenological processes driving tree growth at this ecotone. However, our finding that remote estimates of SDD were statistically similar to tree growth onset at one field site demonstrates that remote sensing holds promise for detecting shifts in phenology in response to climate change at the FTE.


## *Introduction*

Vegetation phenology is strongly linked to the timing and magnitude of carbon (C) sequestration. Therefore, the value of phenological research and monitoring has strengthened in recent years as climatic changes affect the timing of plant growth in many

ecosystems (Jeganathan et al., 2014; Jeong et al., 2011; Wang et al., 2011; White et al., 2005). This shift often results in a longer growing season (earlier start in spring and/or later end in autumn) which potentially increases the amount of wood production (Delpierre et al., 2016b; Lempereur et al., 2015) and aboveground C that can be sequestered over long timescales (Babst et al., 2014; Thomas and Martin, 2012). Despite its importance, the phenology of wood growth is difficult to track especially at large spatial scales, and its response to climate change compared to leaf phenology is relatively understudied (Delpierre et al., 2016a; Ford et al., 2016). Hence, suitable monitoring approaches are needed to ensure that the phenology of tree wood growth can be understood in the context of climate change.

Tree wood growth phenology is particularly important to study in the arctic-boreal region where temperatures are rising 2.5 times faster than the global average (Overland et al., 2018). Within this region is the 13,000 km circumpolar transition zone between the boreal forest and the treeless tundra known as the forest-tundra ecotone (FTE). Because trees growing at the FTE are at the northernmost extent of their global distribution, it has been posited that treeline may be particularly sensitive to subtle changes in climate (Korner, 2012; Malanson et al., 2019), thus providing a valuable opportunity to explore how climatic changes may affect physiological processes such as tree wood growth. In particular, the timing of snow disappearance (with subsequent soil thaw and increases in soil moisture) could affect the length of the growing season for trees at the FTE (Buermann et al., 2013; X. Zhang et al., 2019), where the snow disappearance date (SDD) already appears to be occurring earlier than historically (Callaghan et al., 2011; Pivot et al., 2002; Semmens and Ramage, 2013). How tree wood growth phenology will respond to this is not known, though it will undoubtedly have implications for regional carbon sequestration.

Phenologically sensitive remote sensing techniques could be useful for monitoring the onset of tree wood growth across the FTE. Many studies have demonstrated strong relationships between the onset of photosynthetic activity and remotely sensed vegetation indices (e.g., NDVI) (Beck et al., 2006; Böttcher et al., 2014; Gamon et al., 2016; Vierling et al., 1997)) or solar-induced chlorophyll fluorescence (SIF) (Magney et al., 2019; Parazoo et al., 2018; Pierrat et al., 2021; Walther et al.,

2016). However, to date few studies have explored linkages between remote sensing products and tree wood growth onset, especially in evergreen trees that are common at the FTE and have limited seasonal turnover of foliage.

Recently, Eitel et al. (2020) explored the linkages between foliar-scale observations of the photochemical reflectance index (PRI) and tree wood growth at the FTE. This study utilized point dendrometers affixed to evergreen conifers to determine seasonality of sub-millimeter scale stem growth. Eitel et al. (2020) showed that the PRI signal corresponded closely to daily tree wood growth measurements throughout the growing season, and that PRI was particularly effective at determining the cessation of tree wood growth in late summer. However, PRI did not track tree wood growth onset at the FTE closely. While Eitel et al. (2020) provided a novel method for tracking tree wood growth both during and at the end of the season, a method for detecting tree wood growth onset is still needed to provide an efficient, reliable, and scalable approach for monitoring the seasonality of tree wood growth across the FTE.

Several proxies for detecting tree wood growth onset at coarse spatial scales have been proposed. One such metric is remotely sensed snow disappearance date (SDD). Previous work suggests that the timing of spring snow disappearance corresponds closely with the timing of tree growth onset in evergreen needleleaf trees in the boreal forest (Kirdyanov et al., 2003; Rossi et al., 2011; Vaganov et al., 1999; Yun et al., 2018). Modelling and field studies have shown that physiological processes driving wood growth, including cambial activation and xylogenesis, begin at or immediately after SDD (Rossi et al., 2011; Vaganov et al., 1999). Kirdyanov and colleagues (2003) concluded that areas with later snow disappearance experience a shorter growing season and hence exhibit reduced tree growth due to delayed growth onset. The relationship between SDD and the onset of plant growth has been observed in other vegetation types besides conifers as well, including in tundra systems (Carrer et al., 2019; Cooper et al., 2011; Schmidt et al., 2006). Remote sensing studies further support the idea that there are linkages between SDD and the onset of biomass production, as spectral indices sensitive to the timing of spring green-up have shown a rapid increase after snowmelt (Barichivich et al., 2013; Dye and Tucker, 2003; Pierrat et al., 2021). Finally, Böttcher and colleagues (2014) showed that fractional snow cover dynamics detected by satellites could be an

effective metric for determining and spatially scaling the onset of photosynthetic activity in a boreal conifer forest.

Remote sensing instruments such as the Moderate Resolution Imaging Spectroradiometer (MODIS) mounted on the Aqua and Terra satellites can quantify snow cover and thus SDD across the FTE (Frei et al., 2012; Hall and Riggs, 2007). MODIS snow products are well studied and validated, and are frequently used to monitor changes in snowpack phenology across landscapes (Coll and Li, 2018; Dong et al., 2014; Gudex-Cross et al., 2021; Hall and Riggs, 2007; Huang et al., 2018; Petersky and Harpold, 2018; Selkowitz et al., 2014; Wang et al., 2008; H. Zhang et al., 2019). These products also have a high temporal resolution (1 day), increasing their popularity for satellite-derived snow detection (Riggs et al., 2016). While the use of MODIS snow products may be limited by their relatively coarse spatial resolution (~500 m at nadir, but can vary depending on the sensor view angle), frequent cloud cover interference, and reduced reliability under forested canopies (Frei et al., 2012; Nolin, 2010; O'Leary et al., 2018; Raleigh et al., 2013; Selkowitz et al., 2014), these products can provide a valuable estimate for the end of the snow season at spatial and temporal scales that are not possible to get with *in situ* instruments.

Table 2.1: Site characteristics, along with vegetative cover and climate data, for the two FTE field sites.

| | **AK** | **NWT** |
|---|---|---|
| No. of Plots | 6 | 4 |
| No. of Instrumented Trees | 36 | 24 |
| Latitude | $68^{o}$ N | $68.6^{o}$ N |
| Longitude | $149.8^{o}$ W | $133.7^{o}$ W |
| Elevation | 610 - 760 | 90 - 100 |
| Average Canopy Cover (%) | 19.8 | 13.1 |
| Average Stem Density (stems/$km^2$) | 3.4 | 6 |
| Average Soil Temperature ($^{o}$C) | 1.3 | 0.13 |
| Average Snow Depth (cm) | 37.8 | 36.5 |

The overarching goal of this project was to determine if remotely sensed SDD could be used as a proxy for the onset of tree wood growth in evergreen needleleaf trees growing at the FTE. To accomplish this goal, we tested the following two hypotheses: 1) MODIS-derived SDD ($SDD_{MODIS}$) is not significantly different than in-situ soil temperature-derived SDD ($SDD_{ST}$) at the FTE, thereby suggesting that $SDD_{MODIS}$ is a reliable proxy for in-situ $SDD_{ST}$, and; 2) SDD estimates are not significantly different than the onset of radial growth, thus implying that $SDD_{MODIS}$ could reliably determine the start of tree wood growth in evergreens at the FTE. To test our hypotheses, we used observations from field sites at the North American FTE, leveraging direct measurement of stem wood biomass change with point dendrometers, soil temperature observations, and remotely sensed spectral imaging.

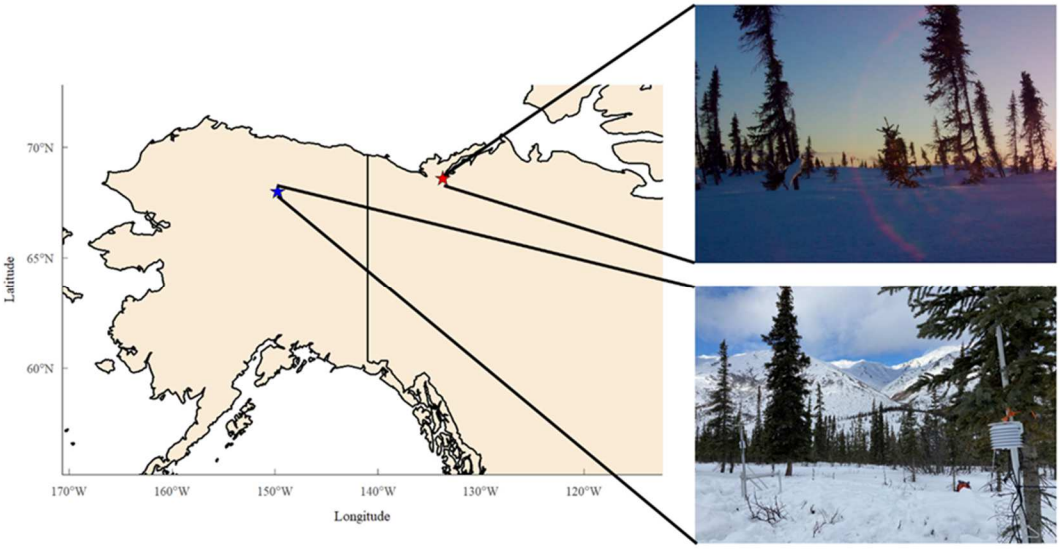


Figure 2.1: Map showing the location of the AK (blue star) and NWT (red star) sites at the forest tundra ecotone, along with images that are representative of both sites.

## *Methods*

### *Study Sites and Observational Setup*

Field data were collected from two FTE study sites during the spring and early summer of 2018-2019 (Figure 2.1). The first site is in the Brooks Range, Alaska, USA (hereafter referred to as AK) and includes six plots located along a north-south transect in the Dietrich River Valley near the Dalton Highway. The area is topographically diverse,

with white spruce (*Picea glauca* (Moench) Voss) and black spruce (*P. mariana* (Mill.) BSP) dominant in the valley bottom and low-stature tundra vegetation growing along the upper slopes. Various willow (*Salix* spp.), birch (*Betula* spp.) and alder (*Alnus* spp) species dominate the understory in the area. Canopy cover among the six plots varied between 9.7% - 28.8%, with an average canopy cover among all six plots of 19.8%.

The second site is in the Mackenzie River Delta near Inuvik, Northwest Territories, Canada (hereafter referred to as NWT) and includes four plots located along a north-south transect. The topography is much less diverse than AK, with white spruce prevalent on the low rolling hills. These trees tend to grow in clumps surrounded by tundra vegetation, with no clear delineation of treeline compared to the AK site. Canopy cover at NWT varied between 2.3% - 40.3%, with an average canopy cover of 13.1% amongst the four plots. At both sites, the first cumulative snowfall generally occurs around October, with snow disappearing some time in May (Semmens and Ramage, 2013; Shi et al., 2015). Table 2.1 includes other important site characteristics for both study sites.

At each plot location, six mature trees were identified and a series of physiological and biophysical sensors were installed at each tree. All instrumented trees ($n$ = 36) in AK were white spruce, while in NWT most of the instrumented trees ($n$ = 18) were white spruce whereas six were black spruce. Sensors included soil temperature probes (RT-1; Meter Group Inc. or 5TM; Meter Group, Inc., USA ) placed at a depth of 10 cm below the soil surface and underneath the canopy of each target tree and point dendrometers (LP-10F; Midori USA) affixed to the tree bole at breast height (137 cm). Point dendrometers measure small changes (micrometer scale) in tree stem radius and have been previously used to accurately determine the onset of tree wood growth (Cruz-Garcia et al., 2019; Eitel et al., 2020; Zweifel et al., 2010). All sensors were connected to a datalogger (CR300; Campbell Scientific, USA or EM50; Meter Group Inc., USA) and continuously collected measurements throughout each study year at either 5- or 20-minute intervals. Data used in this study was collected from 2018 – 2019.

*Snow Disappearance Date*

Two different approaches were used to determine SDD based on *in situ* and satellite measurements. The first method (hereafter referred to $SDD_{ST}$) used plot-level

soil temperature data. During snow-free conditions, surface soil temperatures closely track changes in air temperature, but when snow is present soil temperature decouples from air temperature due to the insulating properties of the snowpack (Lundquist and Lott, 2010; Taras et al., 2002; Tyler et al., 2008) (Figure 2.2). Following previous studies in arctic and alpine ecosystems, $SDD_{ST}$ was defined as the last day in which soil temperatures were stable at approximately 0° C, after which soil temperatures began to fluctuate with air temperatures (Taras et al., 2002).

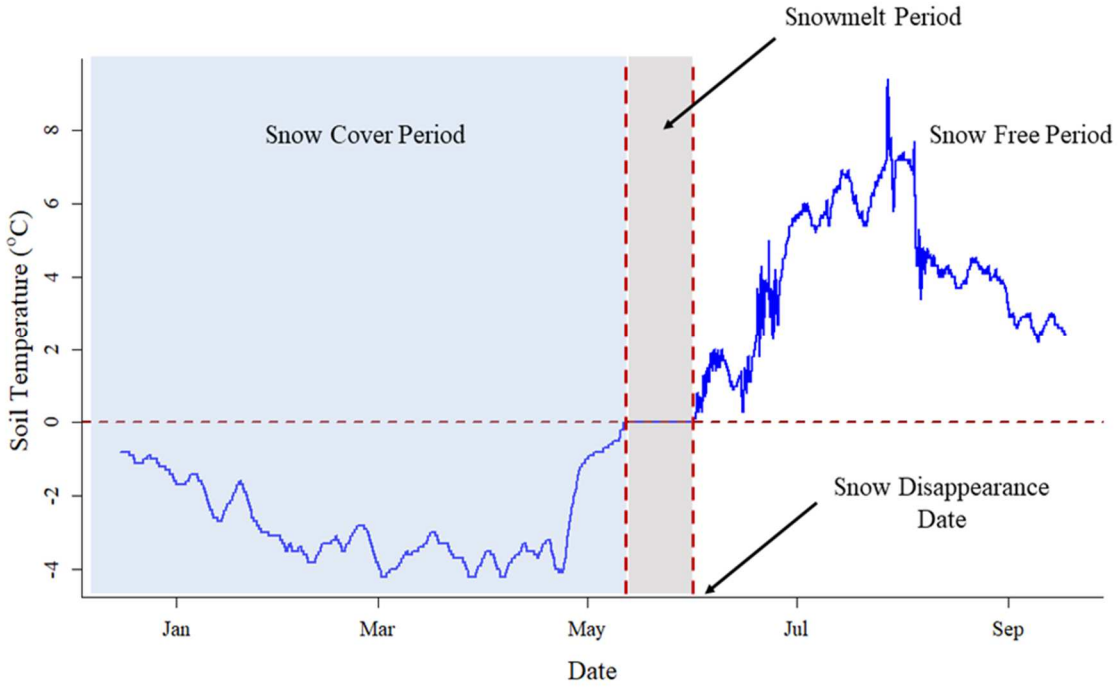


Figure 2.2: Example soil temperature signal from an instrumented tree at the AK field site. The snow cover period, snowmelt period, snow disappearance date, and snow free period are all shown.

The second SDD approach utilized the MODIS MOD10A1 data product (Hall and Riggs, 2016) to find a remotely sensed estimate of SDD ($SDD_{MODIS}$). This product provides daily estimates of NDSI snow cover derived from images collected from the Terra satellite (Riggs et al., 2016). Specifically, the Normalized Difference Snow Index (NDSI), which is derived using the difference in reflectance between the visible-near infrared (0.3 – 1.0 µm) and shortwave-infrared (0.9-1.7 µm) wavelengths, is used to determine snow cover within a pixel (Riggs et al., 2017, 2016). NDSI is calculated using MODIS (from the Terra satellite) band 4 (0.55 µm) and band 6 (1.64 µm):

$$NDSI = \frac{(Band\ 4 - Band\ 6)}{(Band\ 4 + Band\ 6)}$$

A NDSI value of 0.0 indicates snow absence and any NDSI value > 0.0 indicates at least some snow within the pixel (Riggs et al., 2016). While the daily observations provided by the MOD10A1 product are often limited by cloud cover (especially at high latitudes), past studies have shown that snow presence and SDD determined from the MOD10A1 data product do correlate well with ground observations (Ault et al., 2006; Hall and Riggs, 2007; Wang et al., 2008). We analyzed data from the MOD10A1 product collocated with the study sites (5 pixels from AK, 4 pixels from NWT) between Julian Days 121-196 (May 1 – July 15). Due to the heterogeneity inherent in a MODIS pixel at the FTE (where it collects information from both forest and tundra), $SDD_{MODIS}$ was defined as the first day in which the NDSI value for the pixel of interest was equal to 0, indicating complete snowmelt within the pixel (Dong et al., 2014; Huang et al., 2018; H. Zhang et al., 2019).

*Onset of Stem Radial Growth*

Stem radial growth in conifers follows a predictable annual pattern which is useful in deciphering the onset and cessation of growth (Cruz-Garcia et al., 2019; Zweifel et al., 2010). In the early spring and summer stem radius increases until reaching a maximum size in the late summer or fall. After this time, stem radius contracts through the winter and carbon uptake ceases. In late winter the stem contracts to its seasonally minimum radius, after which it begins expanding again. This expansion is indicative of trees refilling stem tissues with water (Drew and Downes, 2009; Zweifel et al., 2006). Irreversible stem radial growth (i.e. woody growth, or xylogensis) begins once the stem radius of the current year surpasses the maximum radius of the previous year and continues through the summer until a new maximum stem radius is reached (Drew and Downes, 2009; Zweifel et al., 2006). Point dendrometers can determine these radial growth patterns as they track minute changes in tree stem radius (De Swaef et al., 2015). Therefore, to determing the onset of radial growth for each study tree in 2018 and 2019 we first found the maximum stem radius reached during the previous year, then following previous work (e.g., Zweifel et al., 2010) we determined the onset of radial growth as the day in which the previous year's maximum stem radius was exceeded.

*Statistical Analysis*

To test our first hypothesis that $SDD_{MODIS}$ is not statistically different from $SDD_{ST}$ we used Mann-Whitney U tests (for non-parametric data) for each site and each year. To test our second hypothesis that SDD is not statistically different than the onset of tree radial growth we again used Mann-Whitney U tests, parsing by SDD method, site, and year. We tested the two sites separately because each site is different in terms of topography, vegetative structure, and snowfall (see Table 2.1). Also, given the increasing criticism of using a significance level threshold (e.g., $\alpha = 0.05$) that dichotomously separates significant from insignificant differences (e.g., see Amrhein et al., 2019), we discuss p-values in the context of "evidence for rejecting the null hypothesis of no difference." All statistical analyses were conducted using the open source software package R version 3.6.2 (R Core Team, 2019). Due to sensor malfunction, insufficient data, etc., some instrumented trees were left out of the analysis. In total, eight and 16 trees distributed across the six plots were included for 2018 and 2019, respectively, at AK. Five and 10 trees across the four plots were included from 2018 and 2019, respectively, at NWT.

Table 2.2: Mean day of year (DOY) and mode for SDDMODIS, SDDST, and radial growth onset for both sites in 2018 and 2019.

| AK FTE | | | | |
|---|---|---|---|---|
| | **2018** | | **2019** | |
| | *Median DOY* | *Mode* | *Median DOY* | *Mode* |
| $SDD_{MODIS}$ | 139 | 139 | 139 | 141 |
| $SDD_{ST}$ | 147 | 147 | 142 | 142 |
| Radial Growth Onset | 170 | 172 | 164 | 164 |
| **NWT FTE** | | | | |
| | **2018** | | **2019** | |
| | *Median DOY* | *Mode* | *Median DOY* | *Mode* |
| $SDD_{MODIS}$ | 152 | 152, 154 | 144 | 144 |
| $SDD_{ST}$ | 172 | NA | 162 | 169 |
| Radial Growth Onset | 127 | NA | 145 | 145 |

## *Results*

### *Comparisons of $SDD_{ST}$ and $SDD_{MODIS}$*

At AK, median SDD occurred between Julian day (DOY) 139 – 147 (May 19 – May 27) in 2018 and 2019 for both methods (Figure 2.3, Table 2.2). $SDD_{MODIS}$ appeared to occur earlier than $SDD_{ST}$ for both 2018 and 2019. There was also a smaller difference between median $SDD_{MODIS}$ and median $SDD_{ST}$ in 2019 (three days) than in 2018 (eight days). The results of the Mann-Whitney U test suggests that there is no difference (alpha $\leq 0.05$) between the distributions of $SDD_{MODIS}$ and $SDD_{ST}$ in 2018 ($p = 0.31$) and in 2019 ($p = 0.05$) (Table 2.3), indicating that $SDD_{MODIS}$ and $SDD_{ST}$ were synchronous.

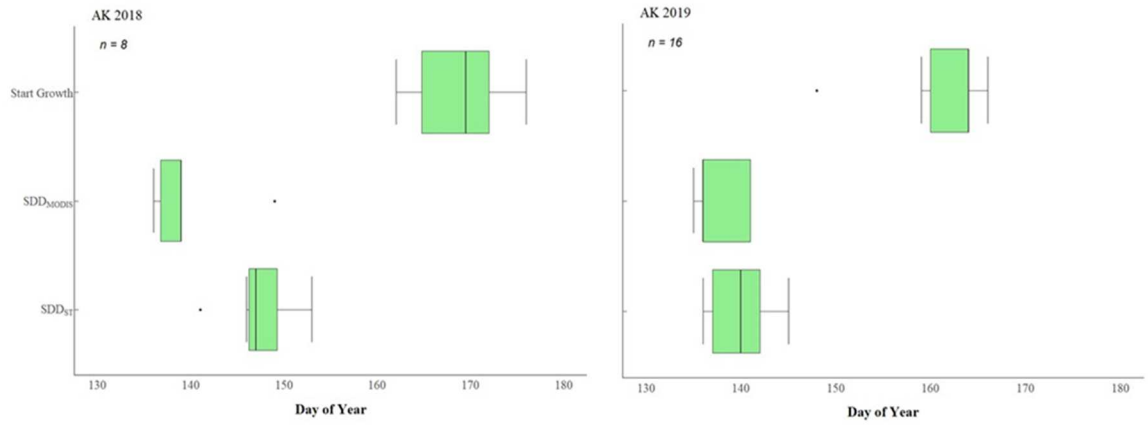


Figure 2.3: Boxplots showing the timing of SDDST, SDDMODIS, and the start of radial growth at the AK site in 2018 (left) and 2019 (right). The black line in each box indicates the median value. The number of trees sampled is also shown.

At NWT, median SDD occurred between DOY 144 – 172 (May 24 – June 21) in 2018 and 2019 for both methods used for determining SDD (Figure 2.4, Table 2.2). Similar to AK, there was variability between years and SDD methods. For example, $SDD_{MODIS}$ occurred earlier than $SDD_{ST}$ in both years, and there was a larger difference between median $SDD_{ST}$ and $SDD_{MODIS}$ in 2018 than in 2019. Median $SDD_{MODIS}$ and $SDD_{ST}$ were separated by 20 days in 2018 and 18 days in 2019. The Mann-Whitney U tests indicated that there was sufficient evidence to reject the null hypothesis of no difference between the distributions of $SDD_{MODIS}$ and $SDD_{ST}$ in both 2018 ($p = 0.01$) and 2019 ($p \leq 0.01$), thus indicating that $SDD_{MODIS}$ and $SDD_{ST}$ were asynchronous (Table

2.3).

*Comparisons Between SDD Estimates and the Start of Radial Growth*

The median tree wood growth onset at AK occurred on DOY 170 (June 19) in 2018 and DOY 164 (June 13) in 2019 (Figure 2.3, Table 2.2). This timing follows the same pattern observed in both SDD estimates, with stem radial growth onset occurring earlier in 2019 than in 2018. However, for both years the start of tree growth occurred approximately two to three weeks after SDD estimates. Results of Mann-Whitney U tests provided strong evidence ($p \leq 0.01$) to reject the statistical null hypothesis of no difference between either $SDD_{MODIS}$ or $SDD_{ST}$ and tree growth onset for both years at the AK site (Table 2.3).

Relative to AK, stem radial growth onset differed more between 2018 and 2019 at NWT (Figure 2.3). On average, radial growth began earlier in 2018 (DOY 127; May 7) than in 2019 (DOY 145; May 25). In addition, in each study year, radial growth began earlier in NWT relative to AK. Radial growth also may have begun at NWT in 2018 before snow had entirely melted (Table 2.2), as radial growth occurred before the median estimate of $SDD_{ST}$ and after that of $SDD_{MODIS}$.

There was statistically significant inter-annual variability when comparing stem radial growth onset and the timing of both SDD estimates at NWT. In 2018, Mann-Whitney U tests showed that radial growth onset was statistically different from the $SDD_{ST}$ ($p = 0.02$) but not from $SDD_{MODIS}$ ($p = 0.14$) (Table 2.3). However, in 2019, neither SDD metric was significantly different from the onset of tree wood growth ($SDD_{ST}$: $p = 0.12$, $SDD_{MODIS}$: $p = 0.08$) (Table 2.3).

Table 2.3: P-values from the Mann-Whitney U tests.

| | p-value | |
|---|---|---|
| **Comparison** | *AK FTE* | *NWT FTE* |
| *Hypothesis 1* | | |
| $SDD_{ST}$ *vs* $SDD_{MODIS}$ *2018* | 0.31 | 0.01 |
| $SDD_{ST}$ *vs* $SDD_{MODIS}$ *2019* | 0.05 | <0.01 |
| *Hypothesis 2* | | |
| $SDD_{ST}$ *vs Radial Growth Onset 2018* | 0.01 | 0.02 |
| $SDD_{ST}$ *vs Start Radial Growth Onset 2019* | < 0.01 | 0.12 |
| $SDD_{MODIS}$ *vs Radial Growth Onset 2018* | <0.01 | 0.14 |
| $SDD_{MODIS}$ *vs Radial Growth Onset 2019* | < 0.001 | 0.08 |

***Discussion***

Previous work exploring relationships between SDD and radial growth (Kirdyanov et al., 2003; Rossi et al., 2011; Vaganov et al., 1999; Yun et al., 2018) suggest that remotely sensed SDD may be a suitable proxy for estimating the onset of stem radial growth. Thus, remotely sensed SDD could represent a key indicator of springtime tree phenology. However, the results of this study showed differences between the timing of $SDD_{MODIS}$ and $SDD_{ST}$, and this asynchrony was also observed when comparing SDD estimates to radial growth onset. It is important to note, however, that there was limited evidence from NWT which indicated that SDD and stem radial growth onset do correspond, thus showing the relationship between SDD and radial

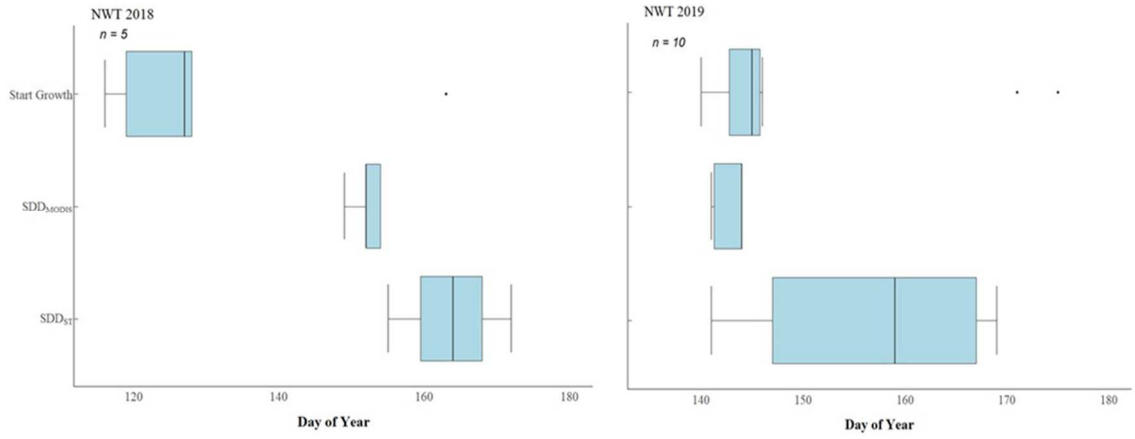


Figure 2.4: Boxplots showing the timing of SDDST, SDDMODIS, and the start of radial growth at the NWT site in 2018 (left) and 2019 (right). The black line in each box indicates the median value. The number of trees sampled is also shown.

growth onset at the FTE may be more complex than initially thought and warrants further investigation.

The differences between $SDD_{MODIS}$ and $SDD_{ST}$ varied by site, yet median $SDD_{MODIS}$ consistently occurred earlier than median $SDD_{ST}$ at both sites, though often only by a few days. The two methods for determining SDD ($SDD_{MODIS}$ and $SDD_{ST}$) produced similar estimates at AK, lending support to Hypothesis 1 that there would be no difference in the timing of these two SDD estimates. However, this was not the case at NWT where $SDD_{MODIS}$ was earlier than $SDD_{ST}$, a finding similar to that of Raleigh et al. (2013). The asynchrony between $SDD_{MODIS}$ and $SDD_{ST}$ is most likely indicative of canopy cover interference. It is documented that MODIS snow products has difficulty detecting snow presence in areas with moderate to high canopy cover (Nolin, 2010; Raleigh et al., 2013), and due to the spatial heterogeneity of the FTE, MODIS pixels undoubtedly contain elements of tundra and forest where SDD often differs (Burles and Boon, 2011; Dickerson-Lange et al., 2017; Lundquist and Lott, 2010; Raleigh et al., 2013). Thus, it is likely that the earlier estimates of $SDD_{MODIS}$ relative to $SDD_{ST}$, particularly at NWT, were due at least in part to a residual snowpack that was hidden from sensor view by tree crowns. In fact, our results suggest that the sub-canopy soil temperature probes at each tree detected the thermal properties associated with this residual sub-canopy snowpack (Figure 2.2), and thus provided later estimates of SDD relative to the remotely sensed estimates. These results further support findings by Raleigh and colleagues (2013) suggesting ground-based sensors are needed to validate results of MODIS snow products, especially in forested environments with spatially heterogenous pixels.

The earlier detection of $SDD_{MODIS}$ when compared to $SDD_{ST}$ could also be caused by variations in snow distribution at NWT. Snow distribution depends on many factors including topography, wind speed and direction, vegetation structure, and insolation (Egli et al., 2011; Hiemstra et al., 2002; Winstral and Marks, 2002). At treeline ecotones, where factors such as vegetation structure, wind speed, and solar radiation can change abruptly, snowpack spatial variability is even more pronounced. This variability then affects melt rates and subsequent snow disappearance in these systems, where snow can often linger in protected sites around trees (Hiemstra et al., 2002). The AK site is considerably different than NWT in topography, vegetation and canopy structure, thus creating potential differences in snowpack characteristics (Table 2.1). Not only could the timing of snow disappearance be changed between the two sites, but the capability of satellite-based products (e.g., $SDD_{MODIS}$) to detect snow disappearance could also be altered. Treeline at AK is more well-defined than NWT: stem density and canopy cover decrease rapidly upon approaching the tundra. Average stem density is also lower at AK

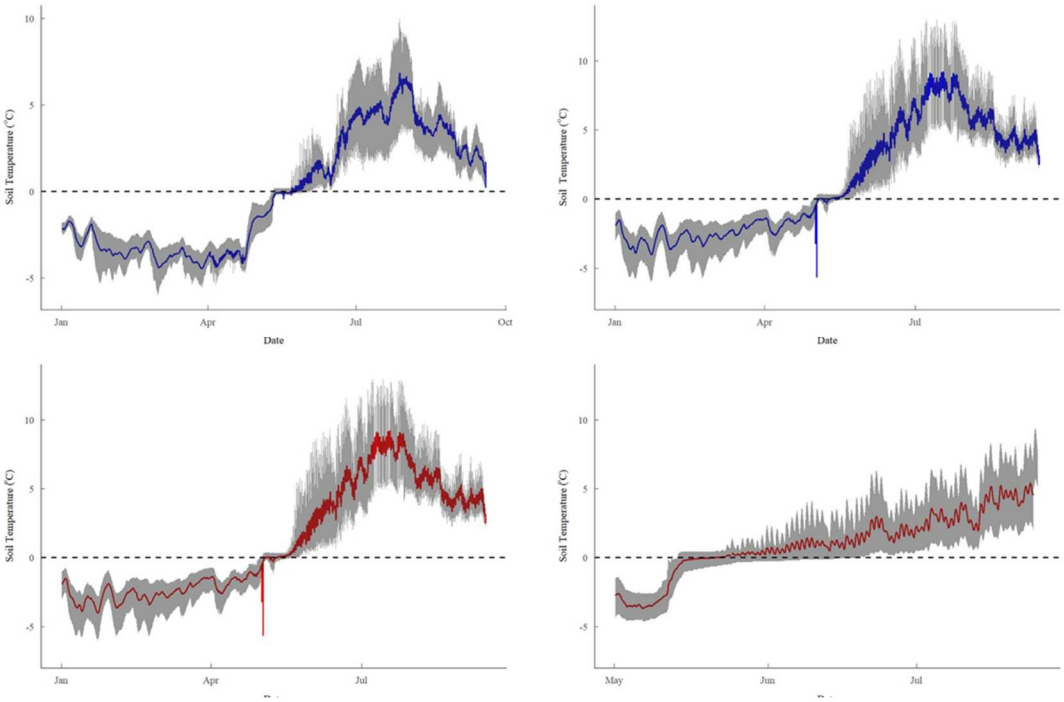


Figure 5: Soil temperature conditions at the AK (blue) and NWT (red) sites during 2018 and 2019. The solid line in each plot indicates the average value, while the gray shaded area indicates the 95th and 5th percentiles of the data.

than at NWT (Table 2.1). This could allow MODIS to more accurately identify SDD when compared to $SDD_{ST}$ at the AK forest-tundra boundary where our instrumented trees are located.

Our second hypothesis stated that SDD estimates would occur at approximately the same time as the onset of stem radial growth in evergreens at the FTE. Results were again somewhat mixed, mostly by site. There was strong evidence that all SDD estimates and radial growth onset were asynchronous at AK, with SDD estimated to have been three to five weeks before trees began growing. At NWT, these results varied mainly by year, with SDD and radial growth onset occurring at similar times in 2019, but not 2018 where radial growth actually began before SDD. These differences in the timing of SDD and radial growth were among the most surprising findings of this study and were contrary to the results of many previous studies in boreal ecosystems (Kirdyanov et al., 2003; Rossi et al., 2011; Vaganov et al., 1999; Yun et al., 2018) that have explored similar phenomena. This discrepancy raises the question: is the timing of snowmelt the key biophysical driver governing the onset of stem radial growth at the FTE, or is it some other variable? More than likely there are a combination of biophysical drivers influencing radial growth onset at high-latitudes, further confounding efforts to find new metrics for monitoring tree growth phenology in these systems (Li et al., 2017; Piao et al., 2019; Treml et al., 2015; Tumajer et al., 2021). While snow melted earlier at the AK site, presumably creating optimal conditions to start growth, perhaps low air or soil temperatures inhibited growth from occurring. There is evidence that low air or soil temperatures in the spring can delay the onset of photosynthesis, stem radial growth onset, and other physiological processes (Ensminger et al., 2004; Reinmann et al., 2018; Reinmann and Templer, 2016; Tanja et al., 2003; Treml et al., 2015). At both field sites there is evidence that soil temperatures remained low (< 5$^{o}$C) through spring and into late June – early July (Figure 2.5). Thus, these low temperatures may have inhibited growth in AK despite the completion of snowmelt. Water availability (from either snow melt or active layer thaw) may also govern tree growth onset, as the expansion of new cambial cells requires water uptake and soil water availability can increase during the snow melt period even when snow is still present (Bowling et al., 2018; Harpold et al., 2015; Zweifel et al., 2000). These possible interactions between snow disappearance, tree

growth onset, and other biophysical variables deserve further study to better understand the uncertainty regarding the hierarchy of environmental drivers affecting growing season phenology at the FTE.

### *Conclusion*

We tested the hypothesis that remotely sensed SDD measurements could be used as a proxy for monitoring the timing of tree growth onset at the FTE, thus providing a novel method for monitoring vegetative phenology in high-latitude coniferous forests. We found intriguing links between remotely sensed SDD and the timing of tree growth onset at the FTE. Overall, results indicate that there are too many confounding factors to use either $SDD_{MODIS}$ or $SDD_{ST}$ as a reliable proxy for tree growth onset at the FTE, though some observations at NWT provide support for this hypothesis. These mixed results highlight the inherent ecological complexities present at the FTE which are difficult to capture with only one biophysical driver. These results suggest scientists should exercise caution when using remotely sensed SDD as a proxy for tree growth in high-latitude systems, where questions still remain about how site characteristics drive potential linkages between tree growth onset and SDD. However, we leverage the apparent limitations of our findings to highlight the key knowledge gaps still present in our understanding of the fundamental biophysical variables driving tree growth at the FTE and across the far north. These gaps must be addressed before we can fully understand and monitor the effect of climate change on vegetation phenology at the FTE.

### *References*

Amrhein, V., Greenland, S., Mcshane, B., 2019. Retire statistical significance. Nature 567, 305–307.

Ault, T.W., Czajkowski, K.P., Benko, T., Coss, J., Struble, J., Spongberg, A., Templin, M., Gross, C., 2006. Validation of the MODIS snow product and cloud mask using student and NWS cooperative station observations in the Lower Great Lakes Region. Remote Sens. Environ. 105, 341–353.

Babst, F., Alexander, M.R., Szejner, P., Bouriaud, O., Klesse, S., Roden, J., Ciais, P., Poulter, B., Frank, D., Moore, D.J.P., 2014. A tree□ring perspective on the terrestrial carbon cycle. Oecologia 176, 307–322. https://doi.org/10.1007/s00442-014-3031-6

Barichivich, J., Briffa, K.R., Myneni, R.B., Osborn, T.J., Melvin, T.M., Ciais, P., Piao, S., Tucker, C., 2013. Large-scale variations in the vegetation growing season and annual cycle of atmospheric $CO_2$ at high northern latitudes from 1950 to 2011. Glob. Chang. Biol. 19, 3167–3183. https://doi.org/10.1111/gcb.12283

Beck, P.S.A., Atzberger, C., Høgda, K.A., Johansen, B., Skidmore, A.K., 2006. Improved monitoring of vegetation dynamics at very high latitudes: A new method using MODIS NDVI. Remote Sens. Environ. 100, 321–334. https://doi.org/10.1016/j.rse.2005.10.021

Böttcher, K., Aurela, M., Kervinen, M., Markkanen, T., Mattila, O., Kolari, P., Metsämäki, S., Aalto, T., Nadir, A., Pulliainen, J., 2014. MODIS time-series-derived indicators for the beginning of the growing season in boreal coniferous forest — A comparison with CO2 flux measurements and phenological observations in Finland. Remote Sens. Environ. 140, 625–638. https://doi.org/10.1016/j.rse.2013.09.022

Bowling, D.R., Logan, B.A., Hufkens, K., Aubrecht, D.M., Richardson, A.D., Burns, S.P., Anderegg, W.R.L., Blanken, P.D., Eiriksson, D.P., 2018. Limitations to winter and spring photosynthesis of a Rocky Mountain subalpine forest. Agric. For. Meteorol. 252, 241–255. https://doi.org/10.1016/j.agrformet.2018.01.025

Buermann, W., Bikash, P.R., Jung, M., Burn, D.H., 2013. Earlier springs decrease peak summer productivity in North American boreal forests. Environ. Res. Lett. 8, 1–10.

Burles, K., Boon, S., 2011. Snowmelt energy balance in a burned forest plot, Crowsnest Pass, Alberta, Canada. Hydrol. Process. 25, 3012–3029. https://doi.org/10.1002/hyp.8067

Callaghan, T. V., Johansson, M., Brown, R.D., Groisman, P.Y., Labba, N., Radionov, V., Barry, R.G., Bulygina, O.N., Essery, R.L.H., Frolov, D.M., Golubev, V.N., Grenfell, T.C., Petrushina, M.N., Razuvaev, V.N., Robinson, D.A., Romanov, P., Shindell, D., Shmakin, A.B., Sokratov, S.A., Warren, S., Yang, D., 2011. The changing face of arctic snow cover: A synthesis of observed and projected changes. Ambio 40, 17–

31.

Carrer, M., Pellizzari, E., Prendin, A.L., Pividori, M., Brunetti, M., 2019. Winter precipitation - not summer temperature - is still the main driver for Alpine shrub growth. Sci. Total Environ. 682, 171–179. https://doi.org/10.1016/j.scitotenv.2019.05.152

Coll, J., Li, X., 2018. Comprehensive accuracy assessment of MODIS daily snow cover products and gap filling methods. ISPRS J. Photogramm. Remote Sens. 144, 435–452. https://doi.org/10.1016/j.isprsjprs.2018.08.004

Cooper, E.J., Dullinger, S., Semenchuk, P., 2011. Late snowmelt delays plant development and results in lower reproductive success in the High Arctic. Plant Sci. 180, 157–167. https://doi.org/10.1016/j.plantsci.2010.09.005

Cruz-Garcia, R., Balzano, A., Cufar, K., Scharnweber, T., Smiljanic, M., Wilmking, M., 2019. Combining Dendrometer Series and Xylogenesis Imagery — DevX , a Simple Visualization Tool to Explore Plant Secondary Growth Phenology. Front. For. Glob. Chang. 2, 1–13. https://doi.org/10.3389/ffgc.2019.00060

De Swaef, T., De Schepper, V., Vandegehuchte, M.W., Steppe, K., 2015. Stem diameter variations as a versatile research tool in ecophysiology. Tree Physiol. 35, 1047–1061. https://doi.org/10.1093/treephys/tpv080

Delpierre, N., Berveiller, D., Granda, E., Dufrêne, E., 2016a. Wood phenology, not carbon input, controls the interannual variability of wood growth in a temperate oak forest. New Phytol. 210, 459–470. https://doi.org/10.1111/nph.13771

Delpierre, N., Vitasse, Y., Chuine, I., Guillemot, J., Bazot, S., Rutishauser, T., Rathgeber, C.B.K., 2016b. Temperate and boreal forest tree phenology: from organ-scale processes to terrestrial ecosystem models. Ann. For. Sci. 73, 5–25. https://doi.org/10.1007/s13595-015-0477-6

Dickerson-Lange, S.E., Gersonde, R.F., Hubbart, J.A., Link, T.E., Nolin, A.W., Perry, G.H., Lundquist, J.D., Roth, T.R., Wayand, N.E., 2017. Snow disappearance timing is dominated by forest effects on snow accumulation in warm winter climates of the Pacific Northwest , United States. Hydrol. Process. 31, 1846–1862. https://doi.org/10.1002/hyp.11144

Dong, J., Ek, M., Hall, D., Peters-Lidard, C., Cosgrove, B., Miller, J., Riggs, G., Xia, Y.,

2014. Using Air Temperature to Quantitatively Predict the MODIS Fractional Snow Cover Retrieval Errors over the Continental United States. J. Hydrometeorol. 15, 551–562. https://doi.org/10.1175/JHM-D-13-060.1

Drew, D.M., Downes, G.M., 2009. The use of precision dendrometers in research on daily stem size and wood property variation: a review. Dendrochronologia 27, 159–172.

Dye, D.G., Tucker, C.J., 2003. Seasonality and trends of snow-cover, vegetation index, and temperature in northern Eurasia. Geophys. Res. Lett. 30, 3–6. https://doi.org/10.1029/2002GL016384

Egli, L., Jonas, T., Grünewald, T., Schirmer, M., Burlando, P., 2011. Dynamics of snow ablation in a small Alpine catchment observed by repeated terrestrial laser scans. Hydrol. Process. 26, 1574–1585. https://doi.org/10.1002/hyp.8244

Eitel, J.U.H., Griffin, K.L., Boelman, N.T., Maguire, A.J., Meddens, A.J.H., Jensen, J., Vierling, L.A., Schmiege, S.C., Jennewein, J.S., 2020. Remote sensing tracks daily radial wood growth of evergreen needleleaf trees. Glob. Chang. Biol. 1–11. https://doi.org/10.1111/gcb.15112

Ensminger, I., Sveshnikov, D., Campbell, D.A., Funks, C., Jansson, S., Lloyd, J., Shibistova, O., Oquist, G., 2004. Intermittent low temperatures constrain spring recovery of photosynthesis in boreal Scots pine forests. Glob. Chang. Biol. 10, 995–1008. https://doi.org/10.1111/j.1365-2486.2004.00781.x

Ford, K.R., Harrington, C.A., Bansal, S., Gould, P.J., St. Clair, J.B., 2016. Will changes in phenology track climate change? A study of growth initiation timing in coast Douglas-fir. Glob. Chang. Biol. 22, 3712–3723. https://doi.org/10.1111/gcb.13328

Frei, A., Tedesco, M., Lee, S., Foster, J., Hall, D.K., Kelly, R., Robinson, D.A., 2012. A review of global satellite-derived snow products. Adv. Sp. Res. 50, 1007–1029. https://doi.org/10.1016/j.asr.2011.12.021

Gamon, J.A., Huemmrich, K.F., Wong, C.Y.S., Ensminger, I., Garrity, S., Hollinger, D.Y., Noormets, A., Peñuelask, J., 2016. A remotely sensed pigment index reveals photosynthetic phenology in evergreen conifers. Proc. Natl. Acad. Sci. U. S. A. 113. https://doi.org/10.1073/pnas.1606162113

Gudex-Cross, D., Keyser, S.R., Zuckerberg, B., Fink, D., Zhu, L., Pauli, J.N., Radeloff,

V.C., 2021. Winter Habitat Indices (WHIs) for the contiguous US and their relationship with winter bird diversity. Remote Sens. Environ. 255, 112309. https://doi.org/10.1016/j.rse.2021.112309

Hall, D.K., Riggs, G.A., 2016. MODIS/Terra Snow Cover Daily L3 Global 500m SIN Grid, Version 6. Boulder, Colorado. https://doi.org/https://doi.org/10.5067/MODIS/MOD10A1.006

Hall, D.K., Riggs, G.A., 2007. Accuracy assessment of the MODIS snow products. Hydrol. Process. 21, 1534–1547. https://doi.org/10.1002/hyp

Harpold, A.A., Molotch, N.P., Musselman, K.N., Bales, R.C., Kirchner, P.B., Litvak, M., Brooks, P.D., 2015. Soil moisture response to snowmelt timing in mixed-conifer subalpine forests. Hydrol. Process. 29, 2782–2798. https://doi.org/10.1002/hyp.10400

Hiemstra, C.A., Liston, G.E., Reiners, W.A., 2002. Snow redistribution by wind and interactions with vegetation at upper treeline in the Medicine Bow Mountains, Wyoming, U.S.A. Arctic, Antarct. Alp. Res. 34, 262–273. https://doi.org/10.2307/1552483

Huang, Y., Liu, H., Yu, B., Wu, J., Kang, E.L., Xu, M., Wang, S., Klein, A., Chen, Y., 2018. Improving MODIS snow products with a HMRF-based spatio-temporal modeling technique in the Upper Rio Grande Basin. Remote Sens. Environ. 204, 568–582. https://doi.org/10.1016/j.rse.2017.10.001

Jeganathan, C., Dash, J., Atkinson, P.M., 2014. Remotely sensed trends in the phenology of northern high latitude terrestrial vegetation, controlling for land cover change and vegetation type. Remote Sens. Environ. 143, 154–170. https://doi.org/10.1016/j.rse.2013.11.020

Jeong, S.J., Ho, C.H., Gim, H.J., Brown, M.E., 2011. Phenology shifts at start vs. end of growing season in temperate vegetation over the Northern Hemisphere for the period 1982-2008. Glob. Chang. Biol. 17, 2385–2399.

Kirdyanov, A., Hughes, M., Vaganov, E., Schweingruber, F., Silkin, P., 2003. The importance of early summer temperature and date of snow melt for tree growth in the Siberian Subarctic. Trees. 17, 61–69. https://doi.org/10.1007/s00468-002-0209-z

Körner, C., 2012. Alpine Treelines: Functional Ecology of the Global High Elevation

Tree Limits. Springer Basel.

Lempereur, M., Martin-StPaul, N.K., Damesin, C., Joffre, R., Ourcival, J.M., Rocheteau, A., Rambal, S., 2015. Growth duration is a better predictor of stem increment than carbon supply in a Mediterranean oak forest: Implications for assessing forest productivity under climate change. New Phytol. 207, 579–590.

Li, X., Liang, E., Gričar, J., Rossi, S., Čufar, K., Ellison, A.M., 2017. Critical minimum temperature limits xylogenesis and maintains treelines on the southeastern Tibetan Plateau. Sci. Bull. 62, 804–812. https://doi.org/10.1016/j.scib.2017.04.025

Lundquist, J.D., Lott, F., 2010. Using inexpensive temperature sensors to monitor the duration and heterogeneity of snow-covered areas. Water Resour. Res. 46.

Magney, T.S., Bowling, D.R., Logan, B.A., Grossmann, K., Stutz, J., Blanken, P.D., Burns, S.P., Cheng, R., Garcia, M.A., Köhler, P., Lopez, S., Parazoo, N.C., Raczka, B., Schimel, D., Frankenberg, C., 2019. Mechanistic evidence for tracking the seasonality of photosynthesis with solar-induced fluorescence. Proc. Natl. Acad. Sci. U. S. A. 116, 11640–11645. https://doi.org/10.1073/pnas.1900278116

Malanson, G.P., Resler, L.M., Butler, D.R., Fagre, D.B., 2019. Mountain plant communities: Uncertain sentinels? Prog. Phys. Geogr. Earth Environ. 030913331984387. https://doi.org/10.1177/0309133319843873

Nolin, A.W., 2010. Recent advances in remote sensing of seasonal snow. J. Glaciol. 56, 1141–1150.

O'Leary, D., Hall, D., Medler, M., Flower, A., 2018. Quantifying the early snowmelt event of 2015 in the Cascade Mountains, USA by developing and validating MODIS-based snowmelt timing maps. Front. Earth Sci. 12, 693–710. https://doi.org/10.1007/s11707-018-0719-7

Overland, J., Dunlea, E., Box, J.E., Corell, R., Forsius, M., Pawlak, J., Reiersen, L., Wang, M., Group, M.R., Environment, G., Foundation, T., Main, V., Observatory, G., 2018. The Urgency of Arctic Change. Polar Sci.

Parazoo, N.C., Arneth, A., Pugh, T.A.M., Smith, B., Steiner, N., Luus, K., Commane, R., Benmergui, J., Stofferahn, E., Liu, J., Rödenbeck, C., Kawa, R., Euskirchen, E., Zona, D., Arndt, K., Oechel, W., Miller, C., 2018. Spring photosynthetic onset and net CO2 uptake in Alaska triggered by landscape thawing. Glob. Chang. Biol. 24,

3416–3435. https://doi.org/10.1111/gcb.14283

Petersky, R., Harpold, A., 2018. Now you see it, now you don't: a case study of ephemeral snowpacks and soil moisture response in the Great Basin, USA. Hydol. Earth Syst. Sci. 22, 4891–4906.

Piao, S., Liu, Q., Chen, A., Janssens, I.A., Fu, Y., Dai, J., Liu, L., Lian, X., Shen, M., Zhu, X., 2019. Plant phenology and global climate change: Current progresses and challenges. Glob. Chang. Biol. 25, 1922–1940. https://doi.org/10.1111/gcb.14619

Pierrat, Z., Nehemy, M.F., Roy, A., Magney, T., Parazoo, N.C., Laroque, C., Pappas, C., Sonnentag, O., Grossmann, K., Bowling, D.R., Seibt, U., Ramirez, A., Johnson, B., Helgason, W., Barr, A., Stutz, J., 2021. Tower□Based Remote Sensing Reveals Mechanisms Behind a Two□phased Spring Transition in a Mixed□Species Boreal Forest. J. Geophys. Res. Biogeosciences 126, 1–20.

Pivot, F.C., Kergomard, C., Duguay, C.R., 2002. Use of passive-microwave data to monitor spatial and temporal variations of snow cover at tree line near Churchill, Manitoba, Canada. Ann. Glaciol. 34, 58–64.

Raleigh, M.S., Rittger, K., Moore, C.E., Henn, B., Lutz, J.A., Lundquist, J.D., 2013. Ground-based testing of MODIS fractional snow cover in subalpine meadows and forests of the Sierra Nevada. Remote Sens. Environ. 128, 44–57.

R Core Team, 2019. R: A language and environment for statistical computing. https://www.R-project.org/.

Reinmann, A.B., Susser, J.R., Demaria, E.M.C., Templer, P.H., 2018. Declines in northern forest tree growth following snowpack decline and soil freezing. Glob. Chang. Biol. 420–430. https://doi.org/10.1111/gcb.14420

Reinmann, A.B., Templer, P.H., 2016. Reduced Winter Snowpack and Greater Soil Frost Reduce Live Root Biomass and Stimulate Radial Growth and Stem Respiration of Red Maple (Acer rubrum) Trees in a Mixed-Hardwood Forest. Ecosystems 19, 129–141. https://doi.org/10.1007/s10021-015-9923-4

Riggs, G.A., Hall, D.K., Román, M.O., 2017. Overview of NASA's MODIS and Visible Infrared Imaging Radiometer Suite ( VIIRS ) snow-cover Earth System Data Records. Earth Syst. Sci. Data 9, 765–777.

Riggs, G.A., Hall, D.K., Román, M.O., 2016. MODIS Snow Products Collection 6 User

Guide 1–66.

Rossi, S., Morin, H., Deslauriers, A., 2011. Multi-scale influence of snowmelt on xylogenesis of black spruce. Arctic, Antarct. Alp. Res. 43, 457–464. https://doi.org/10.1657/1938-4246-43.3.457

Schmidt, N.M., Baittinger, C., Forchhammer, M.C., 2006. Reconstructing Century-Long Snow Regimes Using Estimates of High Arctic Salix arctica Radial Growth. Arctic, Antarct. Alp. Res. 38, 257–262.

Selkowitz, D.J., Forster, R.R., Caldwell, M.K., 2014. Prevalence of pure versus mixed snow cover pixels across spatial resolutions in alpine environments. Remote Sens. 6, 12478–12508. https://doi.org/10.3390/rs61212478

Semmens, K.A., Ramage, J.M., 2013. Recent changes in spring snowmelt timing in the Yukon River basin detected by passive microwave satellite data. Cryosph. 7, 905–

Shi, X., Marsh, P., Yang, D., 2015. Warming spring air temperatures, but delayed spring streamflow in an Arctic headwater basin. Environ. Res. Lett. 10, 64003.

Tanja, S., Berninger, F., Vesala, T., Markkanen, T., Hari, P., Mäkelä, A., Ilvesniemi, H., Hänninen, H., Nikinmaa, E., Huttula, T., Laurila, T., Aurela, M., Grelle, A., Lindroth, A., Arneth, A., Shibistova, O., Lloyd, J., 2003. Air temperature triggers the recovery of evergreen boreal forest photosynthesis in spring. Glob. Chang. Biol. 9, 1410–1426. https://doi.org/10.1046/j.1365-2486.2003.00597.x

Taras, B., Sturm, M., Liston, G.E., 2002. Snow – Ground Interface Temperatures in the Kuparuk River Basin, Arctic Alaska: Measurements and Model. J. Hydrometeorol. 3, 377–394.

Thomas, S.C., Martin, A.R., 2012. Carbon content of tree tissues: A synthesis. Forests 3, 332–352. https://doi.org/10.3390/f3020332

Treml, V., Kašpar, J., Kuželová, H., Gryc, V., 2015. Differences in intra-annual wood formation in Picea abies across the treeline ecotone, Giant Mountains, Czech Republic. Trees - Struct. Funct. 29, 515–526. https://doi.org/10.1007/s00468-014-1129-4

Tumajer, J., Kašpar, J., Kuželová, H., Shishov, V. V., Tychkov, I.I., Popkova, M.I., Vaganov, E.A., Treml, V., 2021. Forward Modeling Reveals Multidecadal Trends in Cambial Kinetics and Phenology at Treeline. Front. Plant Sci. 12, 1–14.

https://doi.org/10.3389/fpls.2021.613643

Tyler, S.W., Burak, S.A., Namara, J.P.M.C., Lamontagne, A., Selker, J.S., Dozier, J., 2008. Spatially distributed temperatures at the base of two mountain snowpacks measured with fiber-optic sensors. J. Glaciol. 54, 673–679.

Vaganov, E.A., Hughes, M.K., Kirdyanov, A. V, Schweingruber, F.H., Silkin, P.P., 1999. Influence of snowfall and melt timing on tree growth in subarctic Eurasia. Nature 400, 149–151.

Vierling, L.A., Deering, D.W., Eck, T.F., 1997. Differences in Arctic Tundra Vegetation Type and Phenology as Seen Using Bidirectional Radiometry in the Early Growing Season. Remote Sens. Environ. 4257, 71–82.

Walther, S., Voigt, M., Thum, T., Gonsamo, A., Zhang, Y., Köhler, P., Jung, M., Varlagin, A., Guanter, L., 2016. Satellite chlorophyll fluorescence measurements reveal large-scale decoupling of photosynthesis and greenness dynamics in boreal evergreen forests. Glob. Chang. Biol. 22, 2979–2996.

Wang, X., Piao, S., Ciais, P., Li, J., Friedlingstein, P., Koven, C., Chen, A., 2011. Spring temperature change and its implication in the change of vegetation growth in North America from 1982 to 2006. Proc. Natl. Acad. Sci. 108, 1240–1245.

Wang, X., Xie, H., Liang, T., 2008. Evaluation of MODIS snow cover and cloud mask and its application in Northern Xinjiang , China. Remote Sens. Environ. 112, 1497–1513. https://doi.org/10.1016/j.rse.2007.05.016

White, M.A., Hoffman, F., Hargrove, W.W., Nemani, R.R., 2005. A global framework for monitoring phenological responses to climate change. Geophys. Res. Lett. 32, 1–4. https://doi.org/10.1029/2004GL021961

Winstral, A., Marks, D., 2002. Simulating wind fields and snow redistribution using terrain-based parameters to model snow accumulation and melt over a semi-arid mountain catchment. Hydrol. Process. 16, 3585–3603.

Yun, J., Jeong, S.J., Ho, C.H., Park, C.E., Park, H., Kim, J., 2018. Influence of winter precipitation on spring phenology in boreal forests. Glob. Chang. Biol. 24, 5176–5187. https://doi.org/10.1111/gcb.14414

Zhang, H., Zhang, F., Zhang, G., Che, T., Yan, W., Ye, M., Ma, N., 2019. Ground-based evaluation of MODIS snow cover product V6 across China: Implications for the

selection of NDSI threshold. Sci. Total Environ. 651, 2712–2726.

Zhang, X., Manzanedo, R.D., Orangeville, L.D., Rademacher, T.T., Li, J., Bai, X., Hou, M., Chen, Z., Zou, F., Song, F., Pederson, N., 2019. Snowmelt and early to mid growing season water availability augment tree growth during rapid warming in southern Asian boreal forests. Glob. Chang. Biol. 25, 3462–3471.

Zweifel, R., Eugster, W., Etzold, S., Dobbertin, M., Buchmann, N., Ha, R., 2010. Link between continuous stem radius changes and net ecosystem productivity of a subalpine Norway spruce forest in the Swiss Alps. New Phytol. 187, 819–830.

Zweifel, R., Item, H., Hasler, R., 2000. Stem radius changes and their relation to stored water in stems of young Norway Spruce trees. Trees. 15.

Zweifel, R., Zimmermann, L., Zeugin, F., Newbery, D.M., 2006. Intra-annual radial growth and water relations of trees: Implications towards a growth mechanism. J. Exp. Bot. 57, 1445–1459.

# Chapter 3: Linkages Between Conifer Leaf Temperatures and Stem Radial Variations in Forests of the Intermountain West


***Abstract***

Climate-induced changes to forest hydrologic regimes are affecting key ecosystem processes in subalpine forests across the Intermountain West of North America. Of particular interest is how stem radial variations (SRVs), which measure tree water status and stem radial growth (i.e., carbon storage) are affected by these hydrologic changes. Point dendrometers, which measure SRVs, are an effective means of monitoring both tree water status and radial growth in forests. However, point dendrometers have a practical deployment limit and may not be applicable for monitoring SRVs across broad regions unless they prove scalable. Thus, a key area of research is combining these point dendrometer measurements with remote sensing data to better monitor water stress and tree growth in forests. Leaf temperatures ($T_L$) measured from thermal remote sensing instruments are well-linked to plant water status and could provide an effective method for monitoring SRVs at larger spatial scales given the wide array of remote sensing instruments collecting thermal data. Thus, the main goal of this study was to determine the suitability for using thermal remote sensing measurements as a proxy for daily changes in SRVs in subalpine forests of the Intermountain West. Specifically, we were interested in answering two main questions: Can we use a combination of remote sensing information and environmental variables to predict 1) tree water status, and 2) tree growth? Within Question 2, we also had two sub-questions: 2.1) Can we predict if trees are growing or not, and 2.2) Based on the results of Question 2.1, can we predict the amount of daily growth? We hypothesized that the strength of the relationship between remotely sensed $T_L$ and SRVs would vary depending on the time of day which $T_L$ was measured. We used an existing environmental monitoring network that collected near continuous SRV and $T_L$ measurements through the 2019 – 2021 growing seasons to answer these questions. Results showed that $T_L$, along with other environmental variables, could predict SRVs well, with maximum $R^2$ values between 0.5 – 0.75 for the best models. However, the time of day which $T_L$ was measured also changed the strength of the models considerably. These results show promise for using remotely sensed $T_L$ as a

proxy for daily SRVs. However, there are still key questions that remain, including how well these relationships scale to the coarser spatial scales. However, this project provides a crucial first step in the development of novel methods for monitoring seasonal SRVs and outlines potential future directions.

### *Introduction*

The hydrologic cycle is intimately linked to ecosystem productivity via plant growth. Thus, alterations to hydrologic regimes due to climate change could have lasting repercussions on ecosystems across western North America and particularly on their ability to sequester carbon (Restaino et al., 2016; USGCRP, 2017; Williams et al., 2020). Subalpine forests of the Intermountain West are particularly vulnerable to changes in the hydrologic cycle, as these ecosystems rely on melting winter snowpack for much of their water availability throughout the year (Case et al., 2021; Restaino et al., 2016; Winchell et al., 2016). As the climate continues to change, snow regimes in the region are more variable than they were in the past, often resulting in shallower snowpacks and earlier snow melt (Fyfe et al., 2017; Klos et al., 2014; Mote et al., 2018). How these snowpack changes will affect ecosystem processes (i.e., carbon capture and sequestration) in subalpine forests is therefore of great importance to the resilience of the Intermountain West (Babst et al., 2014; Bowling et al., 2018; Coulthard et al., 2021).

Stem radial variations (SRVs) could provide insight into how climate change induced changes in snow regimes of subalpine forests will affect tree growth and carbon sequestration. SRVs are the temporal patterns of the expansion and contraction of a tree bole. SRVs are mechanistically linked primarily to tree water status and play a critical role in the forest carbon cycle (Dietrich et al., 2018; Preisler et al., 2021; Zweifel et al., 2001). Diurnally, patterns in SRVs are attributable to tree water status. An increasing atmospheric water demand causes a subsequent contraction of the tree stem as water leaves the phloem, cambial cells and newly forming xylem (also called tree water deficit, or TWD), while cells expand and grow during the night and early morning when the atmospheric water demand is much less (Jones, 2014; Steppe et al., 2015; Zweifel et al., 2021, 2016). SRVs can also provide information on intra-annual (i.e., hourly to daily) stem radial growth and subsequent carbon sequestration at seasonal and annual scales

(Drew and Downes, 2009; Steppe et al., 2015). SRVs are highly vulnerable to changes in hydrologic regimes and reductions in water availability could cause declines in processes like stem radial growth (Dietrich et al., 2018). This will adversely affect key ecosystem services like timber production, habitat provisioning for forest dependent fauna, and long-term carbon sequestration. Automated point dendrometers are instruments which offer extremely fine micrometer-level sensitivity (i.e., micrometer) and high temporal resolution and have been applied to monitor drought stress and tree growth in forests and agricultural settings (Fig. 1) (Preisler et al. 2021; Zweifel et al., 2021). However, point dendrometers have a practical deployment limit and may not be applicable for monitoring SRVs across broad regions and ecosystems unless they prove scalable. Thus, improved methods for monitoring how future snow regime changes will affect landscape scale SRVs in subalpine forests of the Intermountain West are urgently needed.

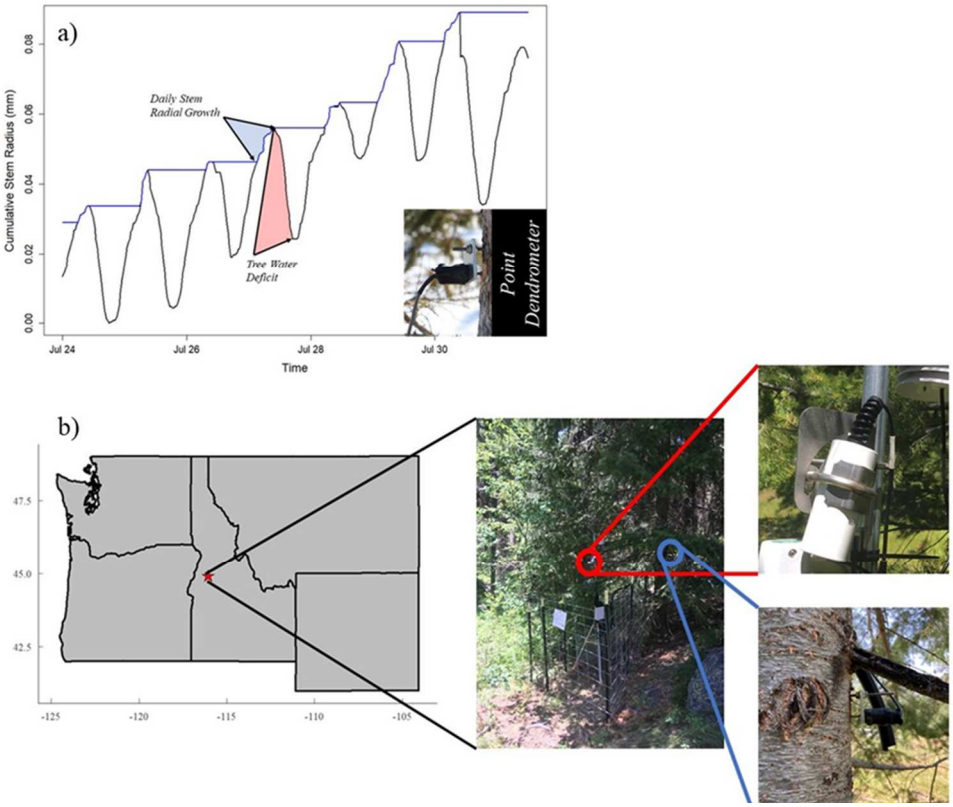


Figure 3.1: a) Stem radial measurements derived from a point dendrometer (inset) at the Nokes Experimental Forest in Central Idaho. The blue line represents the cumulative growth line, while the blue shaded area represents daily stem radial growth, and the red shaded area indicates tree water deficit. b) Map (left) showing the location of the Nokes Experimental Forest (red star) along with an image of a study tree in the forest (middle) and an infrared thermometer (top right) and a point dendrometer (bottom right).

Remote sensing techniques could the gap between spatially limited tree-level measurements regional-scale estimates. Specifically, leaf and canopy temperatures ($T_L$ and $T_C$, respectively) measured using thermal remote sensing have shown strong relationships with intra-annual variability in plant-water status, which is also a primary driver of SRVs. At its most fundamental level, $T_L$ is determined by the leaf energy balance, in which evapotranspiration (ET) plays a foundational role (Campbell and Norman, 1998; Jones, 2014). As a plant transpires, energy is used to evaporate water from the leaf surface which subsequently lowers $T_L$ (Maes and Steppe, 2012; Still et al., 2019). Transpiration occurs during photosynthesis when stomata are open and leaves are assimilating carbon (Jones, 1999; Jones, 2014). Thus, not only is $T_L$ usually regulated by plant-water status, but it is closely linked to photosynthetic activity and carbon uptake (Kim et al., 2016; Niu et al., 2012; Pau et al., 2018; Slot and Winter, 2017).

Table 3.1: Components of the general additive mixed models tested during this project. Models will be referred to by their model names in the left-hand column throughout the text. SRVs stand for stem radial variations.

**SRVs ~ Thermal Remote Sensing + Environmental Covariates**

| *Model Name* | *SRVs* | ***Thermal R.S.*** | *Environmental Covariates* |
|---|---|---|---|
| 1.1 | $TWD_{max}$ | $T_L$ | |
| 1.2 | $TWD_{max}$ | $T_L$ | Photoperiod |
| 1.3 | $TWD_{max}$ | $T_L$ | Photoperiod, PAR |
| 1.4 | $TWD_{max}$ | $T_L$ | Photoperiod, PAR, Soil Moisture |
| 1.5 | $TWD_{max}$ | $T_L$-$T_A$ | |
| 1.6 | $TWD_{max}$ | $T_L$-$T_A$ | Photoperiod |
| 1.7 | $TWD_{max}$ | $T_L$-$T_A$ | Photoperiod, PAR |
| 1.8 | $TWD_{max}$ | $T_L$-$T_A$ | Photoperiod, PAR, Soil Moisture |
| | | | |
| 2.1 | Stem Growth | $T_L$ | |
| 2.2 | Stem Growth | $T_L$ | PAR |
| 2.3 | Stem Growth | $T_L$ | Soil Moisture |
| 2.4 | Stem Growth | $T_L$ | PAR, Soil Moisture |
| 2.5 | Stem Growth | $T_L$-$T_A$ | |
| 2.6 | Stem Growth | $T_L$-$T_A$ | PAR |
| 2.7 | Stem Growth | $T_L$-$T_A$ | Soil Moisture |
| 2.8 | Stem Growth | $T_L$-$T_A$ | PAR, Soil Moisture |

While early research in thermal remote sensing primarily focused on the development of techniques to monitor water use (Idso et al., 1977; H G Jones, 1999), develop stress indices (Idso et al., 1981; Jackson et al., 1981), and schedule irrigation in agricultural environments (Leinonen and Jones, 2004; Page et al., 2018; Struthers et al., 2015), thermography is now widely applied to various environments, including forests. Most of the current work is focused on determining how leaf and canopy temperature measurements vary with canopy structure in different plant functional types (Kim et al., 2018; Leuzinger and Körner, 2007). Studies have also linked canopy temperature to water stress in forest trees (Lapidot et al., 2019; Smigaj et al., 2017), and others have related thermal remote sensing measurements to variables such as net ecosystem exchange, gross primary productivity, and photosynthesis in forests to determine how carbon sequestration may be impacted by canopy temperature measurements (Kim et al., 2016; Niu et al., 2012; Pau et al., 2018). However, to date little work has focused on using thermography to track *intra*-annual patterns in SRVs.

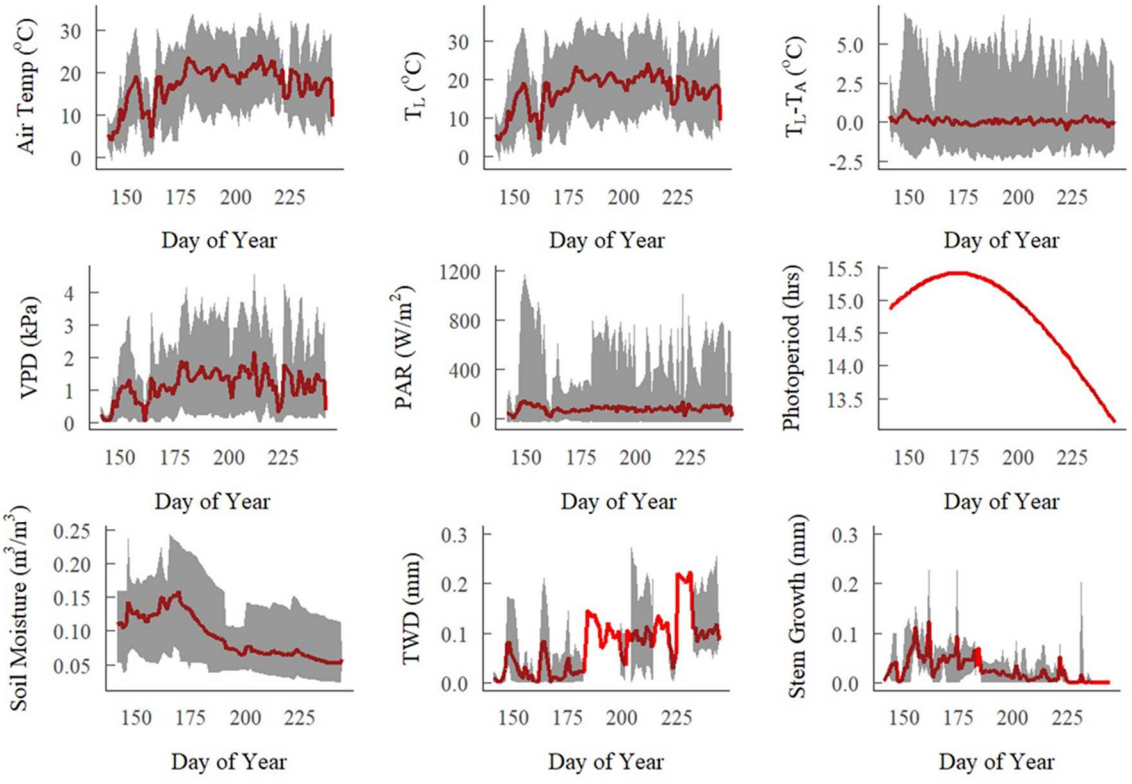


Figure 3.2: Seasonal environmental conditions at the Nokes Experimental Forest during the 2019 – 2021 growing seasons. The red line in each plot indicates the average value, while the gray shaded area indicates the 95th and 5th percentiles of the data.

Thermal remote sensing, with its long history of monitoring plant water status, could provide valuable insights into the effects of hydrologic variability on SRVs which are also mechanistically linked to water availability. However, we know surprisingly little about (1) the strength and type (linear vs nonlinear) of the relationship between remotely sensed thermographic data and SRVs and (2) how this relationship is affected by the timing (e.g., morning vs. afternoon) of thermal remote sensing observations. Hence, there is a clear need to better understand the linkages between thermal remote sensing data and SRVs. This research is especially relevant given the recent (2018) launch of NASA's ECOsystem Spaceborne Thermal Radiometer Experiment on Space Station (ECOSTRESS). This instrument, which measures land surface temperatures (LSTs) every 1 – 3 days, may provide a spaceborne platform for this novel, thermographic approach to monitor the effects of hydrologic variability on SRVs across the Intermountain West (Fisher et al., 2020). However, before thermographic information can be used to track intra-annual SRVs, we need validation studies that leverage thermographic measurements similar to those collected by ECOSTRESS, but at finer spatiotemporal resolution, to track tree-level radial variations which could then enable up-scaling.

Table 3.2: Model results for Question 1, including the $R^2$ values, Akaike Information Criterion (AIC), and time for the best model of each combination of covariates tested.

| *Model Name* | *Model* | $R^2$ | *AIC* | *Time* |
|---|---|---|---|---|
| Model 1.1 | Sqrt. $TWD_{max} \sim f(T_L)$ | 0.32 | 2000.42 | 19:30 |
| Model 1.2 | Sqrt. $TWD_{max} \sim f(T_L)$ + f(photoperiod) | 0.54 | 1702.59 | 20:30 |
| Model 1.3 | Sqrt. $TWD_{max} \sim f(T_L)$ + f(photoperiod) + f(PAR) | 0.55 | 1682.437 | 20:30 |
| Model 1.4 | Sqrt. $TWD_{max} \sim f(T_L)$ + f(photoperiod) + f(PAR) + f(soil moisture) | 0.75 | 1271.905 | 21:00 |
| Model 1.5 | Sqrt. $TWD_{max} \sim f(T_L\text{-}T_A)$ | 0.34 | 2501.06 | 13:00 |
| Model 1.6 | Sqrt. $TWD_{max} \sim f(T_L\text{-}T_A)$ + f(photoperiod) | 0.56 | 2057.037 | 15:30 |
| Model 1.7 | Sqrt. $TWD_{max} \sim f(T_L\text{-}T_A)$ + f(photoperiod) + f(PAR) | 0.61 | 1995 | 15:30 |
| Model 1.8 | Sqrt. $TWD_{max} \sim f(T_L\text{-}T_A)$ + f(photoperiod) + f(PAR) + f(soil moisture) | 0.75 | 2447.824 | 15:30 |

The main goal of this study is to determine the suitability for using thermal remote sensing as a proxy for measuring daily changes in SRVs in subalpine forests of the Intermountain West. Specifically, we were interested in answering two main questions:

Can we use a combination of remote sensing information and environmental variables to predict 1) tree water status, and 2) tree growth? Within Question 2, we also had two sub-questions: 2.1) Can we predict if trees are growing or not, and 2.2) Based on the results of Question 2.1, can we predict the amount of daily growth? We hypothesized that the strength of the relationship between remotely sensed $T_L$ and SRVs would vary depending on the time of day which $T_L$ was measured. The results of this project will help inform future efforts to utilize airborne and spaceborne thermographic products for monitoring SRVs in conifer forests of the Intermountain West.

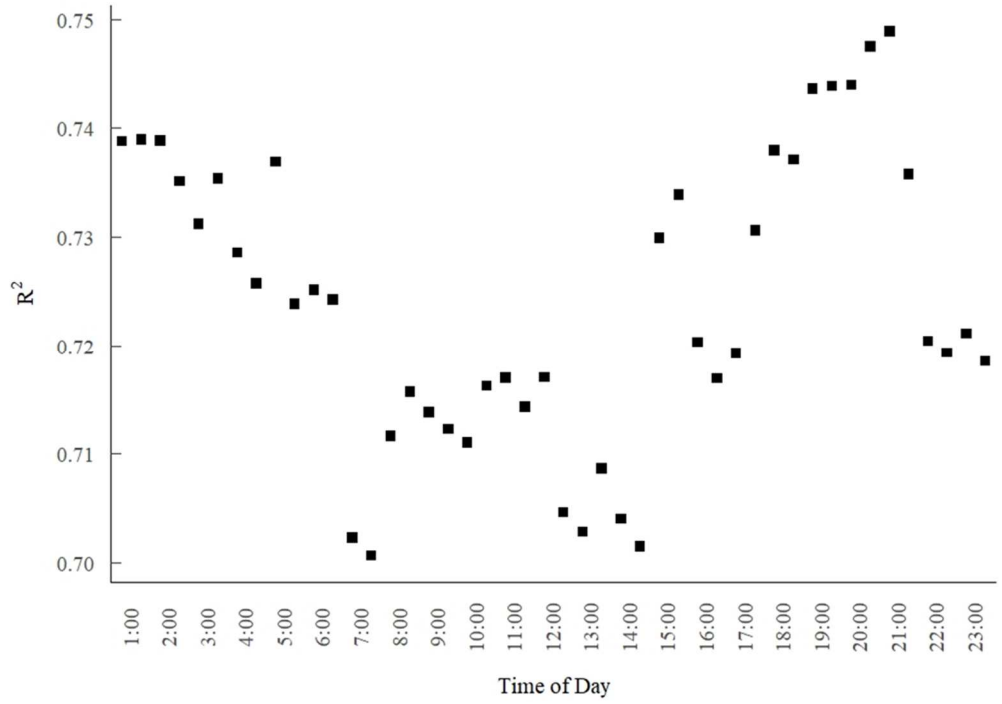


Figure 3.3: $R^2$ values for Model 1.4 ($Sqrt.TWD_{max} \sim f(T_L) + f(photoperiod) + f(PAR) + f(soil\ moisture)$) at each 30-minute interval which $T_L$ was measured.

## *Methods*

### *Study Site*

Data for this project were collected from an existing *in-situ* monitoring network in the Nokes Experimental Forest located near McCall Idaho (Figure 3.1). The area is mostly mixed subalpine conifer forest with ponderosa pine (*Pinus ponderosa* subsp. *Ponderosa*), Douglas fir (*Pseudotsuga menziesii* var. *glauca*), grand fir (*Abies grandis*),

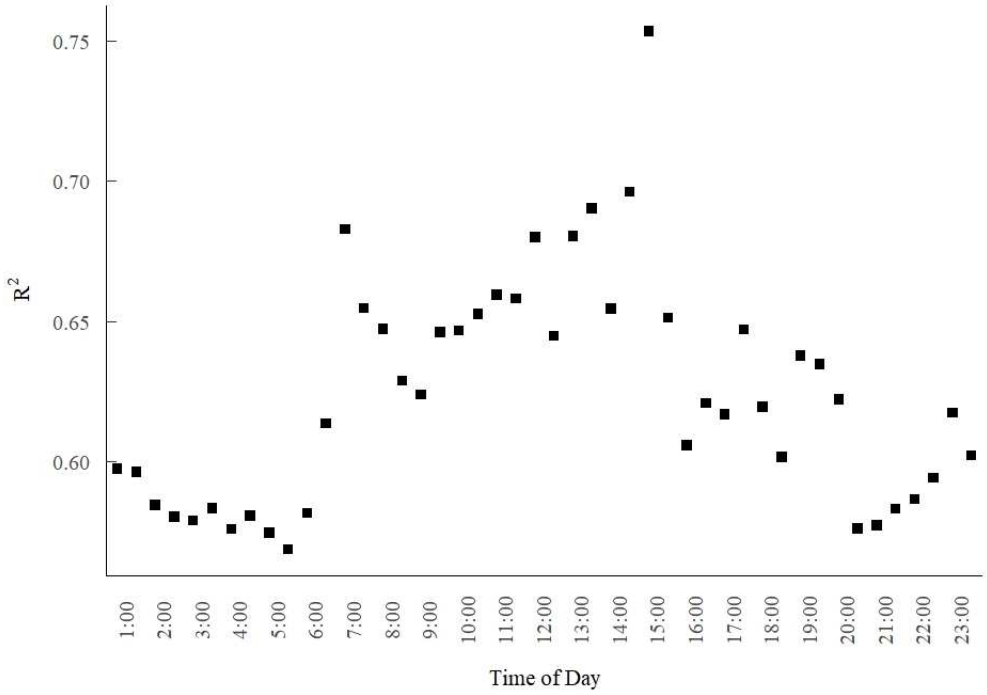


Figure 3.4: $R^2$ values for Model 1.8 ($Sqrt.TWD_{max} \sim f(T_L\text{-}T_A) + f(photoperiod) + f(PAR) + f(soil\ moisture)$) at each 30-minute interval which $T_L$-$T_A$ was measured.

western larch (*Larix occidentalis*), and lodgepole pine (*Pinus contorta* subsp. *latifolia*). Elevation is approximately 1500 m and the forest is characterized by warm, dry summers and cold, wet winters with most of the annual precipitation falling as snow. Snow cover generally lasts from November – May each year (USDA NRCS). Soils across the forest generally consist of several centimeters of coarse plant material with sandy loam underneath (Soil Survey Staff).

The monitoring network was established in spring/summer 2019 and consisted of 10 instrumented trees (five Douglas firs and five grand firs). Instrumented trees were distributed across the forest and vary widely in terms of aspect, surrounding canopy cover, and position within the forest canopy. Several instruments were installed at each tree, including an infrared thermometer (SIF-411, Apogee Instruments, Logan, UT) to measure $T_L$ and point dendrometers (LP-10F, Midori, USA) to monitor SRVs. Infrared thermometers were installed at a height of approximately 2 m and were checked to ensure that foliage of the study tree was maximized within each sensor's field of view. Point dendrometers were installed by carefully scraping off the outer layer of bark and then mounting the sensor on the north side of the tree at breast height (i.e., 1.37 meters) (Eitel

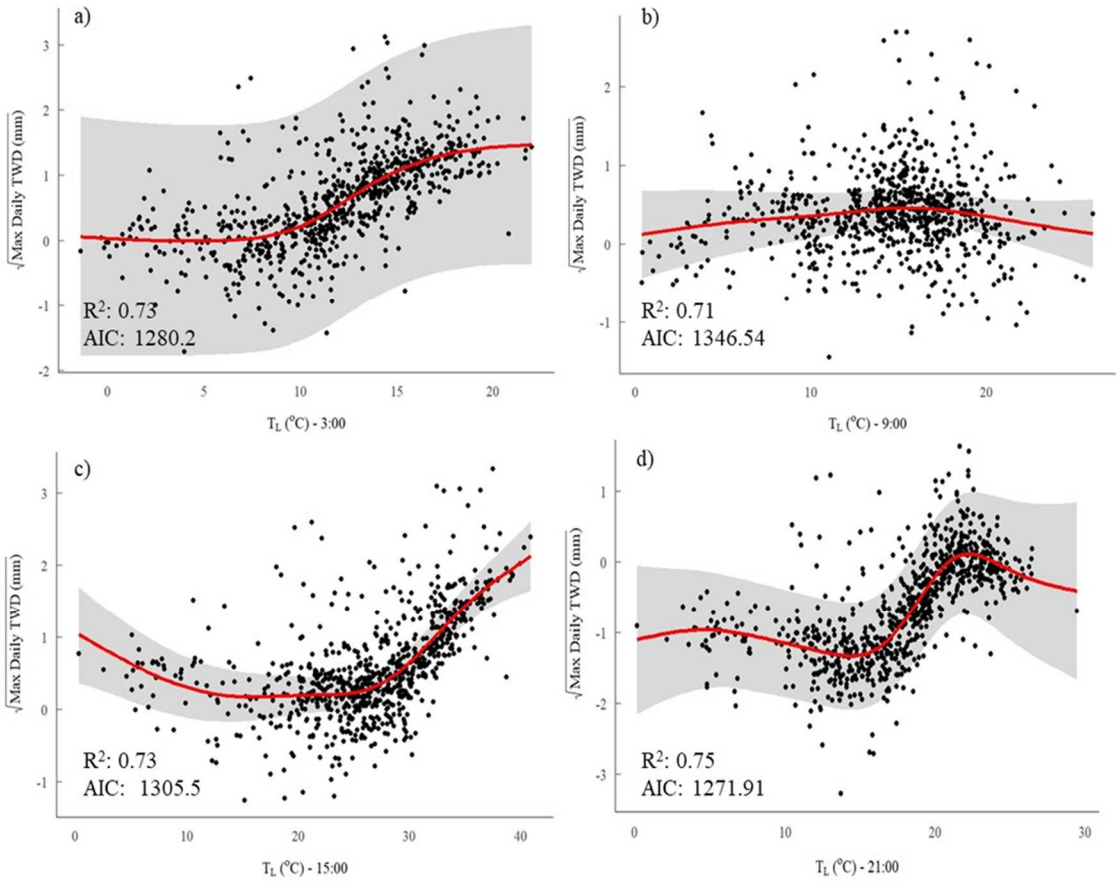


Figure 3.5: Smooth curves for Model 1.4 with $T_L$ measured every 6 hours. $TWD_{max}$ was transformed using a square root transformation to ensure model assumptions were met.

et al., 2020). Other sensors at each tree include a portable weather station (ATMOS14, METER, Pullman, WA) which tracks air temperature, vapor pressure deficit, and air pressure, along with soil moisture/temperature probes (5TM; Meter Group, Inc., USA). All sensors were connected to a ZL6 datalogger (METER, Pullman WA) and set to measure every 10-15 minutes through the growing season. Due to sensor malfunction, data from eight of the 10 trees collected during the 2019, 2020, and 2021 growing seasons were used during analysis.

*Data Processing*

Diurnally, SRVs can be detrended into either TWD or daily stem radial growth (Fig. 1). TWD occurs as the stem contracts during the day and is a measure of tree water stress (Zweifel et al., 2005). Daily stem radial growth occurs as the stem begins to expand once again and surpasses its previous maximum radial value (Zweifel et al., 2016). Unlike TWD, which occurs daily, stem radial growth only occurs when environmental

conditions (e.g., VPD, soil moisture, etc.) are favorable and typically only during the night/early morning hours (Zweifel et al., 2021). We used the 'treenetproc' R package to process the SRV measurements from each instrumented tree (Knüsel et al., 2021).This package converts the raw SRV values into three measurements of interest: stem radius, TWD, and cumulative annual growth. Specifically, TWD is a measure of how much the stem has contracted from its maximum growth value. Cumulative annual growth shows the incremental increase in stem radius from the initial radius at the beginning of the season. The maximum daily TWD ($TWD_{max}$), which indicates the tree at its most water-stressed point, was then found for each tree per day using the calculated TWD values. We calculated mean daily stem growth by finding the average cumulative stem growth for each day during the growing season, and then finding the difference between the current and previous days' growth values. $TWD_{max}$ was used to answer Question 1 while mean daily stem growth was used to answer Question 2.

While conifer $T_L$ measured from the infrared thermometer can provide information on tree water status, we also calculated the leaf-air temperature difference ($T_L$- $T_A$) (Johnson and Smith, 2008). This is another thermal based stress metric which can provide better insight into a tree's stomatal activity (and thus, carbon uptake) (Hoffmann et al., 2016; Osroosh et al., 2015; Ruidong et al., 2019). $T_L$ and $T_L$- $T_A$ were calculated for every half-hour interval through the day, providing 46 observations per tree per day (times 0:00 and 0:30 were not available due to data errors). Photoperiod for each day of the data record was also found using the 'insol' package in R (Corripio, 2021). Mean daily soil moisture derived from the *in-situ* soil moisture sensors as well as

Table 3.3: Model results for Question 2, including the $R^2$ values, AIC, and time for the best model of each combination of covariates tested.

| *Model Name* | *Model* | $R^2$ | *AIC* | *Time* |
|---|---|---|---|---|
| Model2.1 | Sqrt.Growth ~ f($T_L$) | 0.14 | 1815.6 | 22:30 |
| Model2.2 | Sqrt.Growth ~ f($T_L$) + f(PAR) | 0.24 | 1738.18 | 21:00 |
| Model2.3 | Sqrt.Growth ~ f($T_L$) + f(soil moisture) | 0.51 | 1451.61 | 9:00 |
| Model2.4 | Sqrt.Growth ~ f($T_L$) + f(PAR) + f(soil moisture) | 0.55 | 1412.21 | 9:00 |
| Model2.5 | Sqrt.Growth ~ f($T_L$-$T_A$) | 0.18 | 1771.13 | 15:30 |
| Model2.6 | Sqrt.Growth ~ f($T_L$-$T_A$) + f(PAR) | 0.25 | 1720.91 | 15:30 |
| Model2.7 | Sqrt.Growth ~ f($T_L$-$T_A$) + f(soil moisture) | 0.51 | 1453.14 | 17:30 |
| Model2.8 | Sqrt.Growth ~ f($T_L$-$T_A$) + f(PAR) + f(soil moisture) | 0.53 | 1425.81 | 9:00 |

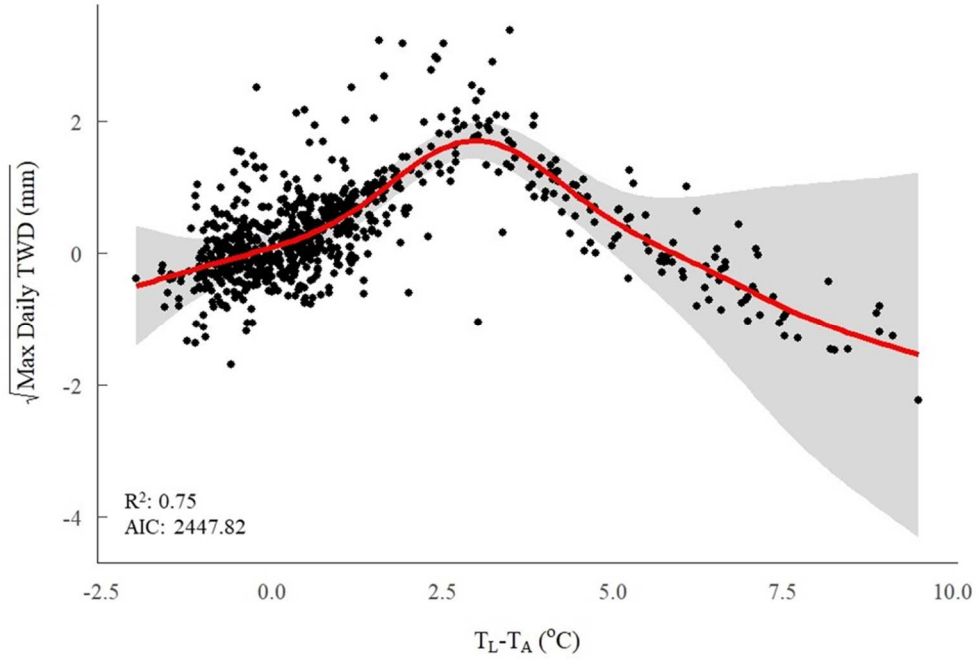


Figure 3.6: Smooth curve for Model 1.8. $TWD_{max}$ was transformed using a square root transformation to ensure model assumptions were met.

photosynthetically active radiation (PAR) measured at each tree were also used as predictor variables during analysis. We collected PAR data using the linear relationship between the hemispherical photochemical reflectance index (PRI) sensors (SRS; METER, Pullman, WA) at each tree and PAR measured with an Apogee SQ100X (Apogee Instruments, Logan, UT). The irradiance at 532 nm (measured from the PRI sensor) was the predictor in the linear model, while measured PAR was the dependent variable. From the resulting model equations, we were able to extrapolate PAR based on irradiance at 532 nm.

*Statistical Analysis*

We used a generalized additive mixed modelling (GAMM) approach to address Question 1 and test how well remotely sensed $T_L$, along other environmental variables, could predict daily $TWD_{max}$. We used a GAMM approach as based on previous work (e.g., Liu et al., 2020; Pau et al., 2018) we assumed the relationship between $T_L$ and $TWD_{max}$ would be nonlinear. We fit models using the 'mgcv' package (Wood, 2011) with $TWD_{max}$ as the dependent variable and a combination of thermal remote sensing and environmental covariates as predictors (Table 3.1). Other environmental covariates tested included air temperature, vapor pressure deficit, and soil temperature. We removed air

temperature and vapor pressure deficit from the models, as these covariates had high collinearity with $T_L$ and were not significant in the model. We also included the tree identification number (tree ID) as a random effect in each of the models. To aid in evaluating the models, each model was given a name, which can be found in Table 3.1. Models with $T_L$, photoperiod, and PAR as covariates were also defined as 'remote-sensing models', as these covariates can all be easily found using widely available remote sensing information.

We created models of daily $TWD_{max}$ using $T_L$ at each half-hour interval through the day (i.e., 01:00, 01:30, 02:00, 02:30… 23:30). We then compared the results of each model using the $R^2$ values and the Akaike Information Criterion (AIC) (Akaike, 1974). Predictors were considered statistically significant if p-values were $\leq 0.05$. To ensure that model assumptions of normality were met, $TWD_{max}$ observations were transformed using a square root transformation.

We used a logistic regression (Bonney, 1987) to answer Question 2.1 and determine if it was possible to predict days when trees were growing or not. We first found days where daily stem radial growth was > 0 (indicating growth) and labelled these days as "1" for growth, while days where daily stem radial growth = 0 (indicating no growth) were labelled "0" for no growth. We then fit logistic regression models where the probability of growth was the dependent variable while remotely sensed $T_L$, photoperiod, and other environmental variables were predictors. A classification table was used to find the accuracy of the models and we also found the thresholds of each predictor for which growth was expected to occur. These results directly informed the analysis for Question 2.2.

Question 2.2 asked whether we could predict how much daily stem radial growth occurred on days where growth was predicted. We thus first used the logistic regression model from Question 2.1 to filter the dataset to only include days on which the probability of stem radial growth was $\geq 0.5$. We then used a GAMM approach similar to Question 1, except with daily stem radial growth as the dependent variable. All other components of the model were the same as those created in Question 1 (Table 3.1), and we also used the same criteria to evaluate the strength of the models. Tree ID was also included as a random effect in the models.

***Results***

*Site conditions*

Air temperatures across all three growing seasons ranged from -1.8ºC to 35.2ºC, with an average air temperature of 18.0ºC (Figure 3.2). Air temperatures generally increased during the early part of the growing season until about day of year (DOY) 200 (July 18/19), at which time air temperatures began a general downward trend. This seasonal pattern was also observed with VPD (Figure 3.2).

$T_L$ varied between -2.04ºC & 42.7ºC with a mean value of 18.1ºC across the period of record. Seasonally $T_L$ showed a trend similar to air temperature and VPD, increasing early season followed by general decreases late in the growing season (Figure 3.2). $T_L$- $T_A$ remained consistent through the growing season around 0ºC with a mean of 0.07ºC, indicating that $T_L$ tracked air temperatures well throughout the season. However, leaves did deviate from air temperatures with a maximum $T_L$- $T_A$ value of 12.8ºC and a minimum of -4.7ºC.

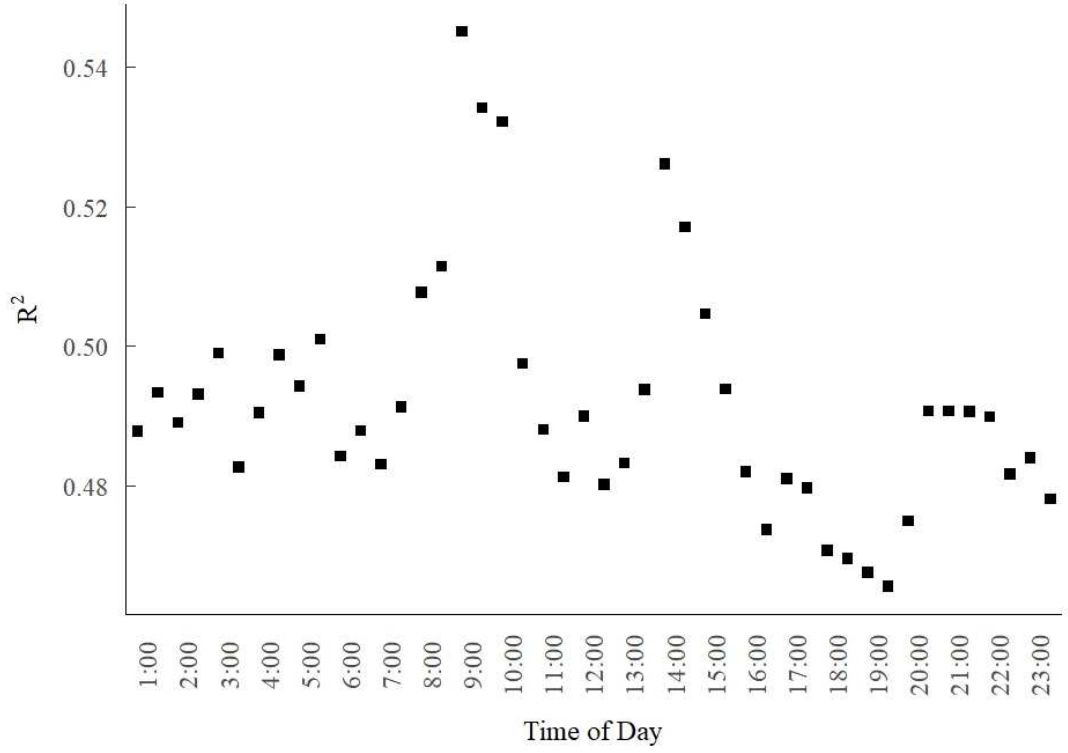


Figure 3.7: $R^2$ values for Model 2.4 (Sqrt.Growth ~ f ($T_L$) + f (PAR) + f (soil moisture)) at each 30-minute interval which $T_L$ was measured.

Soil moisture increased in the early season until approximately DOY 175, at

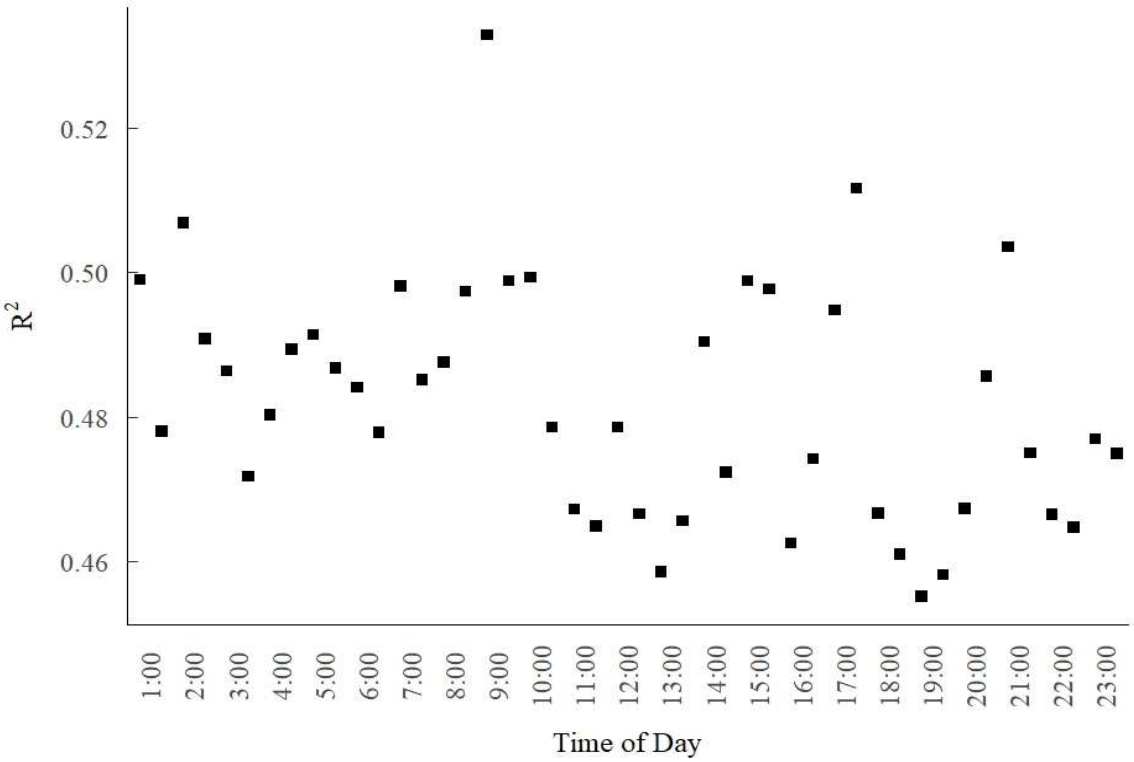


Figure 3.8: $R^2$ values for Model 2.8 (Sqrt.Growth ~ f ($T_L$-$T_A$) + f (PAR) + f (soil moisture)) at each 30-minute interval which $T_L$-$T_A$ was measured.

which time it began decreasing (Figure 3.2). This trend was also observed in stem radial growth where growth was generally highest before DOY 175 and minimal after this date. There were occasional increases in $TWD_{max}$ before DOY 175 (when stem radial growth was highest) but values generally remained < 0.1 mm. $TWD_{max}$ did show an observable increase, however, after DOY 175 after which it generally increased steadily through the remainder of the season.

It is also important to note that the study area, along with much of the Intermountain West, underwent a severe drought during the 2021 growing season (NDMC et al., 2021). At the Nokes Experimental Forest, the highest recorded air temperatures, as well as mean VPD and $T_L$ values in the period of observation were observed during summer 2021.

*Question 1*

Models using a combination of either $T_L$ (Model 1.4) or $T_L$- $T_A$ (Model 1.8), photoperiod, PAR, and mean daily soil moisture were best at predicting $TWD_{max}$ (Table 3.2). These models explained 75% of the observed variability. Remote sensing-based

models (Models 1.2, 1.3, 1.6, 1.7) captured between 56% - 60% of the observed variability when $T_L$- $T_A$ was a covariate and 54% - 55% of the variability in models where $T_L$ was a predictor. Overall, $R^2$ values were similar between models using $T_L$ or $T_L$- $T_A$, though AIC values for Models 1.1 – 1.4 were consistently less than Models 1.5 – 1.8. Models 1.1 and 1.5, which only used a $T_L$ metric as a covariate explained up to 32% - 34% of the observed variance.

Model strength also varied depending on the time-of-day $T_L$ was measured (Figure 3.3). For Models 1.1 – 1.4 more variance was explained when $T_L$ was measured in the evening (19:30 – 21:00) than any other time of day. TWD also appeared to be more sensitive to $T_L$ during the early morning and evening hours than during any other time of day. Models 1.5 – 1.8 explained more of the observed variance when $T_L$- $T_A$ was measured around early afternoon (13:00 – 15:30), and showed a pattern where TWD seemed more sensitive to $T_L$- $T_A$ measured during this midday period than any other time

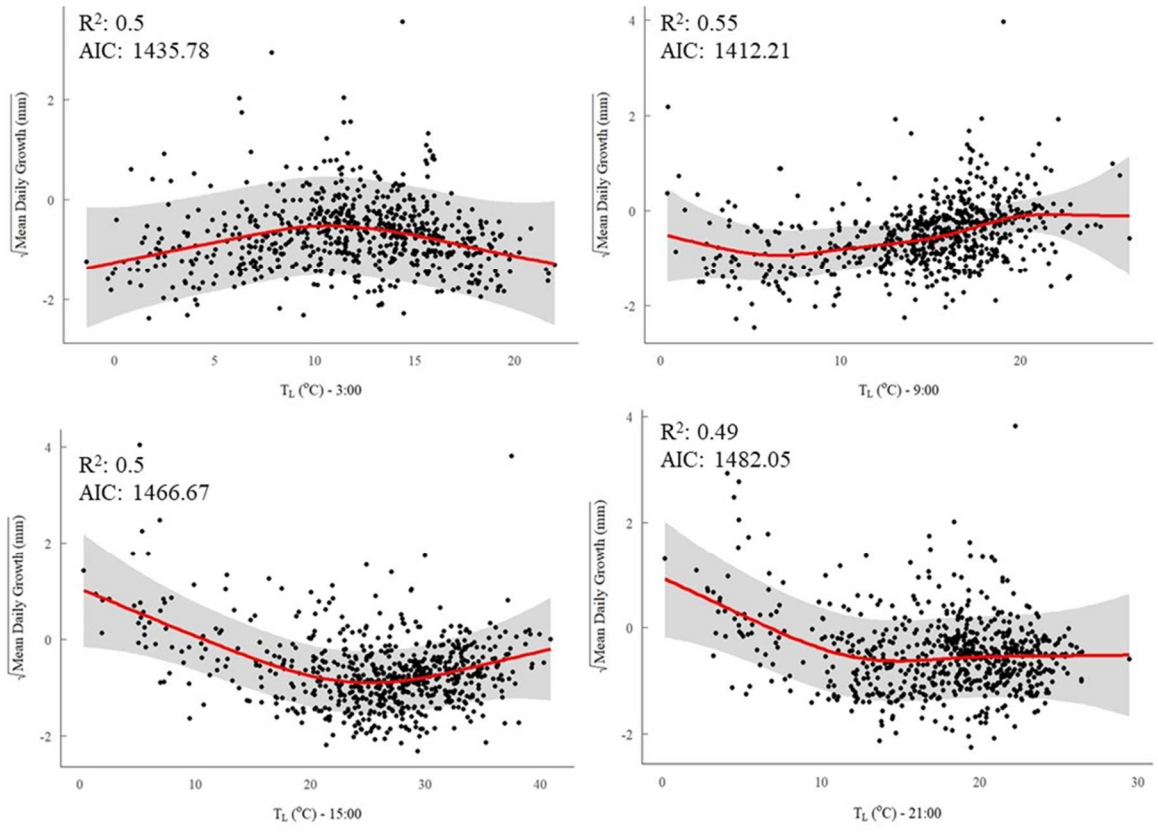


Figure 3.9: Smooth curves for Model 2.4 with $T_L$ measured every 6 hours. Stem growth was transformed using a square root transformation to ensure model assumptions were met.

of day (Figure 3.4).

When examining the smoothing curves for models best predicting $TWD_{max}$, models using $T_L$ as a covariate showed a clear threshold where $TWD_{max}$ values increased as $T_L$ met and exceeded a particular temperature threshold. For Models 1.1 – 1.4 this temperature threshold was approximately 15ºC (Figure 3.5d). However, this threshold value varied depending on the time which $T_L$ was measured (Figure 3.5). In Models 1.5 – 1.8 $TWD_{max}$ increased as $T_L$- $T_A$ increased. There was again a threshold value, however, and when this $T_L$- $T_A$ threshold was reached $TWD_{max}$ values begin to decrease (Figure 3.6).

*Question 2*

Results of the logistic regression model showed that days with growth could be predicted well by photoperiod alone. Using a classification table, we found the probability of growth through 3 growing seasons could be predicted with 79% accuracy. Model results also showed that growth was only predicted to occur on days where photoperiod ≥ 14.1 hours. Based on these results the remaining dataset was adjusted to only include days where photoperiod was ≥ 14.1 hours.

Models using $T_L$ (Model 2.4) or $T_L$- $T_A$ (Model 2.8), PAR and mean daily soil moisture best predicted daily stem radial growth based on the $R^2$ and AIC values (Table 3.3). These models at best explained 55% of the observed variance. Remote sensing-based models (Models 2.1, 2.2, 2.5, 2.6) explained between 14% - 25% of the observed variance. Models 2.1 and 2.5 only explained 14% - 18% of the variability. There were not large differences in the strength of each model regardless of whether $T_L$ or $T_L$- $T_A$ was used as a predictor.

The time of day which measurements were collected also affected the strength of the models. Models that included soil moisture as a predictor generally had higher $R^2$ values in the morning (9:00) than other times of the day. Models just including $T_L$ or $T_L$- $T_A$ as a predictor had better $R^2$ values in the midafternoon or at night (see Model 2.1 and 2.5 in Table 3.3). As a whole Models 2.1 – 2.4 showed trends with higher $R^2$ values in the morning and evening (Figure 3.7), while Models 2.5 – 2.8 had higher $R^2$ values in the morning and midafternoon (Figure 3.8).

Smoothing curves for the best models predicting stem radial growth vary

depending on the predictor variables used to predict growth as well as the time that $T_L$ was measured. When looking at the smooth curves for Model 2.4, stem growth seems to increase slightly with increasing temperatures (Figure 3.9). However, this pattern changes in the afternoon as stem growth begins decreasing with increasing temperatures. At low $T_L$ there is a steep decline in stem radial growth, but it appears that $T_L$ reaches a threshold where stem growth remains steady or increases slightly with increasing $T_L$. The $T_L$ value where this threshold occurs varies depending on the time. Smooth curves for Models 2.5-2.8 also vary. Model 2.8 shows more linear relationships, with stem growth decreasing slightly with increasing $T_L$- $T_A$ in the morning, while stem growth generally increases with increasing $T_L$- $T_A$ in the afternoon (Figure 3.10).

***Discussion***

The results of this project show promise in using thermal remote sensing to track changes in SRVs of subalpine forests across the Intermountain West. Models using a combination of $T_L$ and other environmental covariates were able to capture up to three-quarters of the observed variability when predicting $TWD_{max}$ and just over half the variability when predicting stem radial growth. When predicting $TWD_{max,}$ models using $T_L$- $T_A$ appeared to be slightly more sensitive than models using $T_L$, though these differences were not large and we did not test for statistical significance. Whereas $T_L$ can be influenced by air temperatures, $T_L$- $T_A$ corrects for air temperature effects and can provide better insight into plant water stress. Results from other studies have also found $T_L$- $T_A$ and other thermal metrics to be more sensitive to water stress than $T_L$ alone (Dhillon et al., 2014; Smith, 1978). However, it is important to recognize that models using $T_L$ still explained much of the observed variability and could be better suited for remotely based monitoring of SRVs than $T_L$-$T_A$ as many spaceborne instruments (e.g., ECOSTRESS) measure land surface temperatures (LST), which is analogous to $T_L$, but do not measure $T_A$. Hence, in order to calculate $T_L$-$T_A$ at scales comparable to ECOSTRESS, meteorological reanalysis data would be needed.

Data acquisition timing was another key factor for predicting SRVs. Plots of $R^2$ values clearly showed diurnal patterns in the observed variability (Figures 3.3-3.4 and 3.7-3.8). When predicting $TWD_{max}$, models typically showed the highest $R^2$ values in the afternoon and early evening, the time when water potentials are usually at their minimum and the tree is under the greatest water stress (Figures 3.3-3.4) (Lo Gullo and Salleo, 1988; Meinzer et al., 1986). Models predicting stem radial growth also showed diurnal patterns, with $R^2$ values typically peaking in the morning or late evening hours, which corresponds with the times of day when atmospheric water demand is lowest and the transpiration stream should be relaxed (Figures 3.7-3.8) (Ziaco and Biondi, 2018; Zweifel et al., 2021, 2001). This result is similar to the findings of Zweifel et al. (2021), who discovered that stem radial growth is most sensitive to environmental conditions during the early morning hours. Acquisition timing also affected the predicted smooth curves for each model (particularly for models including $T_L$ as a covariate), both in the shape of the curve and the temperatures which SRVs were sensitive to changes (Figures 3.5-3.6 and

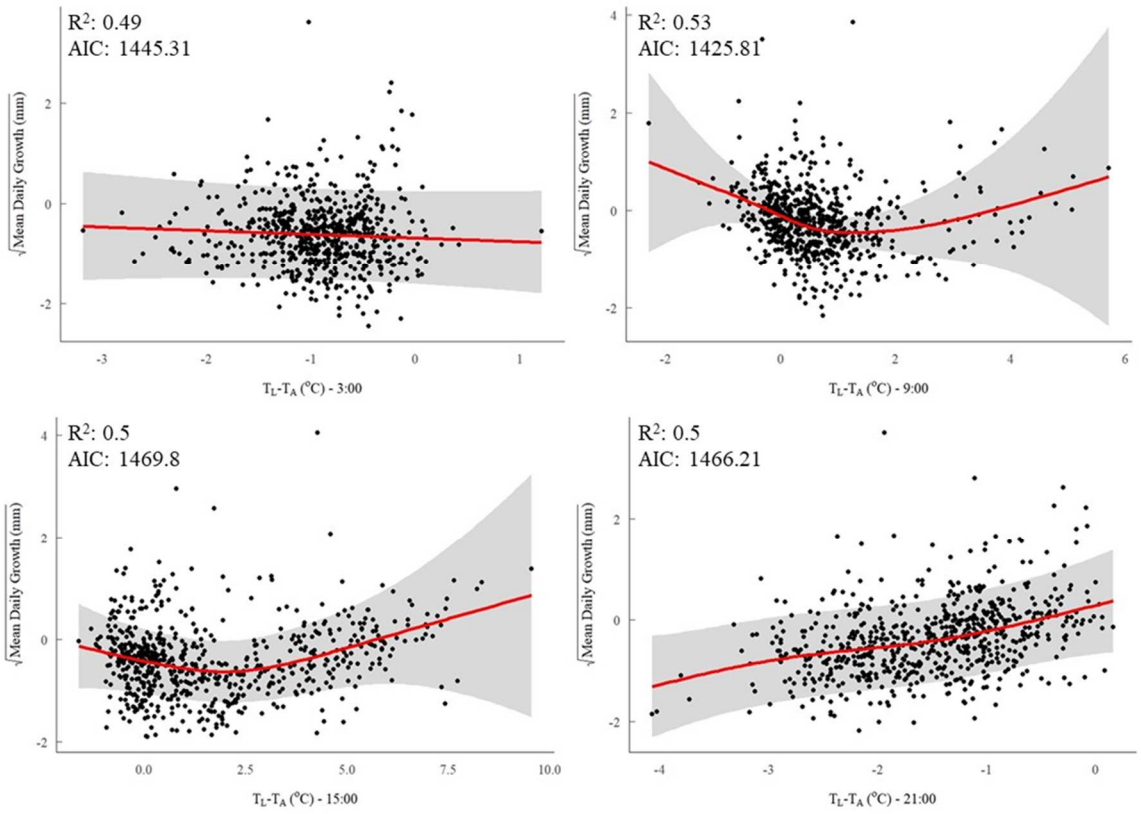


Figure 3.10: Smooth curves for Model 2.8 with $T_L$- $T_A$ measured every 6 hours. Stem growth was transformed using a square root transformation to ensure model assumptions were met.

3.9-3.10). This could impact future efforts to use remotely sensed $T_L$ to track SRVs, as many remote sensing platforms (e.g., ECOSTRESS) have irregular overpass times (Fisher et al., 2020; Hulley et al., 2017) and could collect measurements at times when relationships between $T_L$ and SRVs may not be as strong. However, this irregular overpass time also provides an advantage as it can provide insight into the diurnal patterns and dynamics of key ecosystem processes that may not be detectable in instruments with set overpass times (Xiao et al., 2021). The results of this study show that the relationships between daily SRVs and $T_L$ can vary depending on the time which $T_L$ is measured. Thus, this study demonstrates how important it is to detect these diurnal patterns.

While thermal remote sensing shows promise for monitoring SRVs, there are some possible limitations to this approach that still need to be addressed. Namely, these models were not able to detect exact changes in SRVs, as $TWD_{max}$ and stem radial growth values were transformed using a square root transformation to ensure that model assumptions were met. Still, while exact values cannot be obtained these models could provide insight into relative changes of SRVs over time using thermal remote sensing information in an approach similar to the LandTrendr algorithm for Landsat imagery (Kennedy et al., 2010). If spaceborne instruments like ECOSTRESS, which has a revisit frequency of 1 – 5 days (Fisher et al., 2020), are used to collect $T_L$ information then this approach could help estimate relative changes in SRV dynamics in subalpine coniferous forests at diurnal to sub-weekly scales. Other instruments, such as the Moderate Resolution Imaging Spectroradiometer (MODIS) and Landsat, which collect LST data could also be used for tracking SRVs, but with coarser spatial and temporal resolutions than ECOSTRESS.

Another consideration for possible remote sensing methods is how well these models will predict SRVs at coarser spatial scales. This project utilized *in-situ*, shoot-level measurements of $T_L$, which can vary greatly from average canopy temperatures ($T_C$) and LST due to canopy positioning, shading effects, and microclimatic conditions (Johnston et al., 2021). Thus, there still remains a key question: whether the relationships between SRVs and $T_L$ observed in this study will be as strong when using $T_C$ instead of $T_L$. Further vital work is needed to test these models using canopy level data as well as

LST at the scale of a spaceborne instrument pixel.

The best models found that $TWD_{max}$ and stem radial growth were predicted by $T_L$, photoperiod, PAR, and mean daily soil moisture as covariates. Of these predictors, $T_L$, photoperiod, and PAR are relatively easy to obtain from spaceborne instruments with high accuracy and fine spatial resolution. Soil moisture measurements, however, can be quite complex and difficult to obtain using remote sensing techniques, as soil moisture is highly spatially variable and can be confounded by factors such as vegetation cover and soil physical properties (Cosby et al., 1984; D'Odorico et al., 2007). Indeed, remote sensing techniques can only measure surface level soil moisture, which may not be the most ecologically relevant information (Karthikeyan and Mishra, 2021). Despite these limitations, however, there have been advancements in our ability to measure soil moisture using remote sensing techniques, including with thermal remote sensing instruments (Babaeian et al., 2019). However retrieval of high resolution soil moisture data is still a key challenge that will need to be addressed to before further application of these results.

Even with these current limitations, this study presents novel linkages between diurnal SRVs and remotely sensed $T_L$ in subalpine coniferous forests of the Intermountain West. These results could inform efforts to develop new approaches for monitoring diurnal and seasonal changes in SRVs using thermal remote sensing data across forested regions like the Intermountain West. These efforts will be crucial as hydrologic regimes continue to change, impacting SRVs and carbon cycling in these forests. This project provides a crucial first step in the development of these novel methods and outlines potential future directions.

***References***

Akaike, H., 1974. A New Look at the Statistical Model Identification. IEEE Trans. Automat. Contr. 19, 716–723. https://doi.org/10.1109/TAC.1974.1100705

Babaeian, E., Sadeghi, M., Jones, S.B., 2019. Ground, Proximal, and Satellite Remote Sensing of Soil Moisture. Rev. Geophys. 57, 530–616.

Babst, F., Alexander, M.R., Szejner, P., Bouriaud, O., Klesse, S., Roden, J., Ciais, P., Poulter, B., Frank, D., Moore, D.J.P., 2014. A tree □ ring perspective on the

terrestrial carbon cycle. Oecologia 176, 307–322. https://doi.org/10.1007/s00442-014-3031-6

Bonney, G.E., 1987. Logistic Regression for Dependent Binary Observations. Biometrics 43, 951–973.

Bowling, D.R., Logan, B.A., Hufkens, K., Aubrecht, D.M., Richardson, A.D., Burns, S.P., Anderegg, W.R.L., Blanken, P.D., Eiriksson, D.P., 2018. Limitations to winter and spring photosynthesis of a Rocky Mountain subalpine forest. Agric. For. Meteorol. 252, 241–255. https://doi.org/10.1016/j.agrformet.2018.01.025

Campbell, G.S., Norman, J.M., 1998. An Introduction to Environmental Biophysics, 2nd ed. Springer Science+Business Media, New York.

Case, M.J., Johnson, B.G., Bartowitz, K.J., Hudiburg, T.W., 2021. Forests of the future: Climate change impacts and implications for carbon storage in the Pacific Northwest, USA. For. Ecol. Manage. 482, 118886.

Cosby, B.J., Hornberger, G.M., Clapp, R.B., Ginn, T.R., 1984. A Statistical Exploration of the Relationships of Soil Moisture Characteristics to the Physical Properties of Soils. Water Resour. Res. 20, 682–690. https://doi.org/10.1029/WR020i006p00682

Coulthard, B.L., Anchukaitis, K.J., Pederson, G.T., Cook, E., Littell, J., Smith, D.J., 2021. Snowpack signals in North American tree rings. Environ. Res. Lett. 16, 34037. https://doi.org/10.1088/1748-9326/abd5de

D'Odorico, P., Caylor, K., Okin, G.S., Scanlon, T.M., 2007. On soil moisture-vegetation feedbacks and their possible effects on the dynamics of dryland ecosystems. J. Geophys. Res. Biogeosciences 112, 1–10. https://doi.org/10.1029/2006JG000379

Dhillon, R., Rojo, F., Roach, J., Upadhyaya, S., Delwiche, M., 2014. A Continuous Leaf Monitoring System for Precision Irrigation Management in Orchard Crops. J. Agric. Mach. Sci. 10, 267–272.

Dietrich, L., Zweifel, R., Kahmen, A., 2018. Daily stem diameter variations can predict the canopy water status of mature temperate trees. Tree Physiol. 38, 941–952. https://doi.org/10.1093/treephys/tpy023

Drew, D.M., Downes, G.M., 2009. The use of precision dendrometers in research on daily stem size and wood property variation: a review. Dendrochronologia 27, 159–172.

Eitel, J.U.H., Griffin, K.L., Boelman, N.T., Maguire, A.J., Meddens, A.J.H., Jensen, J., Vierling, L.A., Schmiege, S.C., Jennewein, J.S., 2020. Remote sensing tracks daily radial wood growth of evergreen needleleaf trees. Glob. Chang. Biol. 1–11. https://doi.org/10.1111/gcb.15112

Fisher, J.B., Lee, B., Purdy, A.J., Halverson, G.H., Dohlen, M.B., Nicholson, K.C., Wang, A., Anderson, R.G., Aragon, B., Arain, M.A., Baldocchi, D.D., Baker, J.M., Barral, H., 2020. ECOSTRESS : NASA ' s Next Generation Mission to Measure Evapotranspiration From the International Space Station Water Resources Research. Water Resour. Res. 56, 1–20. https://doi.org/10.1029/2019WR026058

Fyfe, J.C., Derksen, C., Mudryk, L., Flato, G.M., Santer, B.D., Swart, N.C., Molotch, N.P., Zhang, X., Wan, H., Arora, V.K., Scinocca, J., Jiao, Y., 2017. Large near-Term projected snowpack loss over the western United States. Nat. Commun. 8, 1–7. https://doi.org/10.1038/ncomms14996

Hoffmann, H., Jensen, R., Thomsen, A., Nieto, H., Rasmussen, J., Friborg, T., 2016. Crop water stress maps for an entire growing season from visible and thermal UAV imagery. Biogeosciences 13, 6545–6563. https://doi.org/10.5194/bg-13-6545-2016

Hulley, G., Hook, S., Fisher, J., Lee, C., 2017. ECOSTRESS, A NASA Earth-Ventures Instrument for studying links between the water cycle and plant health over the diurnal cycle. Int. Geosci. Remote Sens. Symp. 2017-July, 5494–5496. https://doi.org/10.1109/IGARSS.2017.8128248

Idso, Sherwood, B., Jackson, R.D., Reginato, R.J., 1977. Remote-Sensing of Crop Yields. Science (80-. ). 196, 19–25.

Idso, S.B., Jackson, R.D., Pinter Jr, P.J., Reginato, R.J., Hatfield, J.L., 1981. Normalizing the Stress-Degree-Day Parameter for Environmental Variability. Agric. Meteorol. 24, 45–55.

Jackson, R.D., Idso, S.B., Reginato, R.J., Pinter, P.J., 1981. Temperature as a Crop Water Stress Indicator. Water Resour. Res. 17, 1133–1138.

Johnson, D.M., Smith, W.K., 2008. Cloud immersion alters microclimate , photosynthesis and water relations in Rhododendron catawbiense and Abies fraseri seedlings in the southern Appalachian Mountains , USA. Tree Physiol. 28, 385–392.

Johnston, M.R., Andreu, A., Verfaillie, J., Baldocchi, D., González-Dugo, M.P., Moorcroft, P.R., 2021. Measuring surface temperatures in a woodland savanna: Opportunities and challenges of thermal imaging in an open-canopy ecosystem. Agric. For. Meteorol. 310. https://doi.org/10.1016/j.agrformet.2021.108484

Jones, H.G., 2014. Plants and Microclimate: A Quantitative Approach to Environmental Plant Physiology, 3rd ed. Cambridge University Press.

Jones, H G, 1999. Use of thermography for quantitative studies of spatial and temporal variation of stomatal conductance over leaf surfaces. Plant, Cell Environ. 22, 1043–1055.

Jones, Hamlyn G, 1999. Use of infrared thermometry for estimation of stomatal conductance as a possible aid to irrigation scheduling 95, 139–149.

Karthikeyan, L., Mishra, A.K., 2021. Multi-layer high-resolution soil moisture estimation using machine learning over the United States. Remote Sens. Environ. 266, 112706. https://doi.org/10.1016/j.rse.2021.112706

Kennedy, R.E., Yang, Z., Cohen, W.B., 2010. Detecting trends in forest disturbance and recovery using yearly Landsat time series: 1. LandTrendr - Temporal segmentation algorithms. Remote Sens. Environ. 114, 2897–2910. https://doi.org/10.1016/j.rse.2010.07.008

Kim, Y., Still, C.J., Hanson, C. V., Kwon, H., Greer, B.T., Law, B.E., 2016. Canopy skin temperature variations in relation to climate, soil temperature, and carbon flux at a ponderosa pine forest in central Oregon. Agric. For. Meteorol. 226–227, 161–173. https://doi.org/10.1016/j.agrformet.2016.06.001

Kim, Y., Still, C.J., Roberts, D.A., Goulden, M.L., 2018. Thermal infrared imaging of conifer leaf temperatures: Comparison to thermocouple measurements and assessment of environmental influences. Agric. For. Meteorol. 248, 361–371.

Klos, P.Z., Link, T.E., Abatzoglou, J.T., 2014. Extent of the rain-snow transition zone in the western U.S. under historic and projected climate. Geophys. Res. Lett. 41, 4560–4568.

Knüsel, S., Peters, R.L., Haeni, M., Wilhelm, M., 2021. Processing and Extraction of Seasonal Tree Physiological Parameters from Stem Radius Time Series. Forests 1–14.

Lapidot, O., Ignat, T., Rud, R., Rog, I., Alchanatis, V., Klein, T., 2019. Use of thermal imaging to detect evaporative cooling in coniferous and broadleaved tree species of the Mediterranean maquis. Agric. For. Meteorol. 271, 285–294. https://doi.org/10.1016/j.agrformet.2019.02.014

Leinonen, I., Jones, H.G., 2004. Combining thermal and visible imagery for estimating canopy temperature and identifying plant stress. J. Exp. Bot. 55, 1423–1431. https://doi.org/10.1093/jxb/erh146

Leuzinger, S., Körner, C., 2007. Tree species diversity affects canopy leaf temperatures in a mature temperate forest. Agric. For. Meteorol. 146, 29–37. https://doi.org/10.1016/j.agrformet.2007.05.007

Liu, N., Deng, Z., Wang, H., Luo, Z., Gutiérrez-Jurado, H.A., He, X., Guan, H., 2020. Thermal remote sensing of plant water stress in natural ecosystems. For. Ecol. Manage. 476, 118433. https://doi.org/10.1016/j.foreco.2020.118433

Lo Gullo, M.A., Salleo, S., 1988. Different strategies of drought resistance in three Mediterranean sclerophyllous trees growing in the same environmental conditions. New Phytol. 108, 267–276.

Maes, W.H., Steppe, K., 2012. Estimating evapotranspiration and drought stress with ground-based thermal remote sensing in agriculture: a review. J. Exp. Bot. 63, 4671–4712. https://doi.org/10.1093/jxb/err313

Meinzer, F.C., Rundel, P.W., Sharifi, M.R., Nilsen, E.T., 1986. Turgor and osmotic relations of the desert shrub Larrea tridentata. Plant. Cell Environ. 9, 467–475.

Mote, P.W., Li, S., Lettenmaier, D.P., Xiao, M., Engel, R., 2018. Dramatic declines in snowpack in the western US. npj Clim. Atmos. Sci. https://doi.org/10.1038/s41612-018-0012-1

National Drought Mitigation Center (NDMC), U.S. Department of Agriculture (USDA), and National Oceanic and Atmospheric Administration (NOAA). 2021. U.S. Drought Monitor. https://droughtmonitor.unl.edu/CurrentMap.aspx. Accessed 12-2-2022.

Niu, S., Luo, Y., Fei, S., Yuan, W., Schimel, D., Law, B.E., Ammann, C., Arain, M.A., Arneth, A., Aubinet, M., Barr, A., Beringer, J., Bernhofer, C., Black, T.A., Buchmann, N., Cescatti, A., Chen, J., Davis, K.J., Dellwik, E., Desai, A.R., Etzold,

S., Francois, L., Gianelle, D., Gielen, B., Goldstein, A., Gu, L., Hanan, N., Helfter, C., Hirano, T., Hollinger, D.Y., Mike, B., Kiely, G., Kolb, T.E., Kutsch, W.L., Lafleur, P., Lawrence, D.M., Lindroth, A., Litvak, M., Loustau, D., Lund, M., Marek, M., Martin, T.A., Matteucci, G., Migliavacca, M., Montagnani, L., Moors, E., Munger, J.W., Oechel, W., Olejnik, J., U, K.T.P., Pilegaard, K., Rambal, S., Spano, D., Stoy, P., Sutton, M.A., Varlagin, A., Scott, R.L., 2012. Thermal optimality of net ecosystem exchange of carbon dioxide and underlying mechanisms. New Phytol. 194, 775–783.

Osroosh, Y., Peters, R.T., Campbell, C.S., 2015. Estimating actual transpiration of apple trees based on infrared thermometry. J. Irrig. Drain. Eng. 141, 1–13. https://doi.org/10.1061/(ASCE)IR.1943-4774.0000860

Page, G.F.M., Liénard, J.F., Pruett, M.J., Moffett, K.B., 2018. Spatiotemporal dynamics of leaf transpiration quantified with time-series thermal imaging. Agric. For. Meteorol. 256–257, 304–314. https://doi.org/10.1016/j.agrformet.2018.02.023

Pau, S., Detto, M., Kim, Y., Still, C.J., 2018. Tropical forest temperature thresholds for gross primary productivity. Ecosphere 9, e02311. https://doi.org/10.1002/ecs2.2311

Preisler, Y., Tatarinov, F., Yakir, D., 2021. Seeking the " point of no return " in the sequence of events leading to mortality of mature trees. Plant. Cell Environ. 44, 1315–1328. https://doi.org/10.1111/pce.13942

Restaino, C.M., Peterson, D.L., Littell, J., 2016. Increased water deficit decreases Douglas fir growth throughout western US forests. Proc. Natl. Acad. Sci. U. S. A. 113, 9557–9562. https://doi.org/10.1073/pnas.1602384113

Ruidong, Z., Zhou, Y., Yue, Z., Chen, X., Cao, X., Ai, X., Jiang, B., Xing, Y., 2019. The leaf-air temperature difference reflects the variation in water status and photosynthesis of sorghum under waterlogged conditions. PLoS One 14, 1–15. https://doi.org/10.1371/journal.pone.0219209

Slot, M., Winter, K., 2017. In situ temperature response of photosynthesis of 42 tree and liana species in the canopy of two Panamanian lowland tropical forests with contrasting rainfall regimes. New Phytol. 214, 1103–1117.

Smigaj, M., Gaulton, R., Suarez, J.C., Barr, S.L., 2017. Use of miniature thermal cameras for detection of physiological stress in conifers. Remote Sens. 9.

Smith, W.K., 1978. Temperatures of Desert Plants: Another Perspective on the Adaptability of Leaf Size. Science (80-. ). 201, 614–616.

Soil Survey Staff, Natural Resources Conservation Service, United States Department of Agriculture. Web Soil Survey. Available online at the following link: http://websoilsurvey.sc.egov.usda.gov/. Accessed 12/5/2021.

Steppe, K., Sterck, F., Deslauriers, A., 2015. Diel growth dynamics in tree stems: Linking anatomy and ecophysiology. Trends Plant Sci.

Still, C., Powell, R., Aubrecht, D., Kim, Y., Helliker, B., Roberts, D., Richardson, A.D., Goulden, M., 2019. Thermal imaging in plant and ecosystem ecology: applications and challenges. Ecosphere 10, e02768. https://doi.org/10.1002/ecs2.2768

Struthers, R., Ivanova, A., Tits, L., Swennen, R., Coppin, P., 2015. Thermal infrared imaging of the temporal variability in stomatal conductance for fruit trees. Int. J. Appl. Earth Obs. Geoinf. 39, 9–17.

USDA Natural Resources Conservation Service. (2021). SNOwpack TELemetry Network (SNOTEL). NRCS. https://data.nal.usda.ov/dataset/snowpack-telemetry-network-snotel. Accessed 2021-12-2.

USGCRP, 2017. Climate Science Special Report: Fourth National Climate Assessment, Volume I. Washington, DC, USA. https://doi.org/10.7930/J0J964J6

Williams, A.P., Cook, E.R., Smerdon, J.E., Cook, B.I., Abatzoglou, J.T., Bolles, K., Baek, S.H., Badger, A.M., Livneh, B., 2020. Large contribution from anthropogenic warming to an emerging North American megadrought. Science (80-. ). 368, 314–318.

Winchell, T.S., Barnard, D.M., Monson, R.K., Burns, S.P., Molotch, N.P., 2016. Earlier snowmelt reduces atmospheric carbon uptake in midlatitude subalpine forests. Geophys. Res. Lett. 43, 8160–8168. https://doi.org/10.1002/2016GL069769.Received

Xiao, J., Fisher, J.B., Hashimoto, H., Ichii, K., Parazoo, N.C., 2021. Emerging satellite observations for diurnal cycling of ecosystem processes. Nat. Plants 7, 877–887. https://doi.org/10.1038/s41477-021-00952-8

Ziaco, E., Biondi, F., 2018. Stem Circadian Phenology of Four Pine Species in Naturally Contrasting Climates from Sky-Island Forests of the Western USA. Forests 9. https://doi.org/10.3390/f9070396

Zweifel, R., Haeni, M., Buchmann, N., Eugster, W., 2016. Are trees able to grow in periods of stem shrinkage? New Phytol. 211, 839–849. https://doi.org/10.1111/nph.13995

Zweifel, R., Item, H., Häsler, R., 2001. Link between diurnal stem radius changes and tree water relations. Tree Physiol. 21, 869–877.

Zweifel, R., Sterck, F., Braun, S., Buchman, N., Eugster, W., Gessler, A., Hani, M., Peters, R.L., Walthert, L., Wilhelm, M., Zieminska, K., Etzold, S., 2021. Why trees grow at night. New Phytol. 1–29. https://doi.org/10.1111/nph.17552

Zweifel, R., Zimmermann, L., Newbery, D.M., 2005. Modeling tree water deficit from microclimate : an approach to quantifying drought stress. Tree Physiol. 25, 147–156.

# Chapter 4: Conclusions

Stem radial growth is an important physiological process in the temperate and boreal forests of North America and influences global water and carbon (C) cycling. Despite this importance, few methods exist to measure intra-annual stem radial growth at landscape and ecosystem level scales. This project sought to remedy this by exploring linkages between 1) remotely sensed snow disappearance date (SDD) estimates and the timing of stem radial growth onset in the spring, and 2) remotely sensed leaf and canopy temperatures ($T_L$ and $T_C$, respectively) and intra-annual stem radial variations (SRVs). While these studies do not present new space-based remote sensing approaches for monitoring stem radial growth, they do lay a vital foundation for future studies to explore the effectiveness of spaceborne instruments to track radial growth.

The results of Chapter 2 showed mixed results when using SDD as a proxy for radial growth onset at the forest-tundra ecotone (FTE). There was limited evidence from the FTE site in the Northwest Territories (NWT) showing that MODIS-derived SDD ($SDD_{MODIS}$) occurred at the same time as radial growth onset. However, different results were seen at the Alaska FTE site (AK), where $SDD_{MODIS}$ and radial growth onset were asynchronous. Results also showed that $SDD_{MODIS}$ and in-situ soil temperature derived SDD estimates ($SDD_{ST}$) were asynchronous as well, suggesting a mismatch between satellite level and ground-based estimates of SDD. These mixed results were contrary to our hypotheses and the findings of past studies (Kirdyanov et al., 2003; Rossi et al., 2011; Vaganov et al., 1999) examining the same phenomenon. However, these results are not wholly unexpected, as past studies have demonstrated that $SDD_{MODIS}$ can struggle to detect snow under forest canopies or other dense vegetation (Raleigh et al., 2013). This could explain the disconnect between $SDD_{MODIS}$ and the onset of stem radial growth at the FTE, where canopy cover is spatially heterogeneous and MODIS pixels are undoubtedly a mixture of forest cover and open tundra. MODIS products may have detected snow cover in the open areas of the pixel while not being able to detect a lingering snowpack underneath the tree canopies, thus determining no snow cover for the pixel. Indeed, the in-situ estimates of snow disappearance indicate the presence of a lingering snowpack underneath the forest canopies, as $SDD_{ST}$ was detected

later than $SDD_{MODIS}$. This could be true particularly for NWT where $SDD_{MODIS}$ was detected earlier than $SDD_{ST}$.

The asynchrony between SDD and radial growth onset, especially at AK, also points to the influence of other biophysical factors besides SDD on the timing of radial growth onset in the spring. Springtime air temperatures, soil temperatures, and photoperiod can all influence radial growth phenology (Ensminger et al., 2004; Parazoo et al., 2018; Tanja et al., 2003). Low air and soil temperatures especially can delay stem radial growth onset in high-latitude and mountain environments where cold conditions can linger for days to weeks after snow disappearance (Reinmann et al., 2018; Reinmann and Templer, 2016). This could have influenced the timing of radial growth onset at the FTE, as soil temperatures did not increase substantially until mid-June – July at both sites. Were these other biophysical factors delaying the radial growth onset so it didn't correspond with SDD? More research is needed into the biophysical drivers of springtime growth phenology of conifers at the FTE to help better contextualize the results from this study.

Chapter 3 explored relationships between leaf level remotely sensed $T_L$ and intra-annual SRVs to better understand if $T_L$ could serve as a proxy for SRVs. Results showed that $T_L$, along with other environmental variables, could predict both tree water deficit and stem radial growth reasonably well through the growing season ($R^2 > 0.5$). However, tree water status was better predicted than stem radial growth, possibly due to the more direct linkage between tree water deficit, $T_L$, and tree water status. The time of day which $T_L$ was measured also influenced the strength of the models, with $T_L$ usually measured in either the morning or the evening best predicting SRVs. This finding has significant potential contributions to any effort to use $T_L$ measured from spaceborne sensors to monitor SRVs, as the timing of data collection will affect the strength of the relationship. Satellite sensors like ECOSTRESS or Landsat 9 may be uniquely situated to monitor this relationship, as they could provide a satellite level glimpse into not only the weekly and seasonal dynamics of SRVs, but also diurnal SRV patterns (Fisher et al., 2020).

While the results of this study were promising, there were also several considerations for future studies. When predicting SRVs, models used a combination of $T_L$ and other environmental variables. These included air temperature, photoperiod,

photosynthetically active radiation (PAR), and average soil moisture. Most of these predictors ($T_L$, photoperiod, PAR) can be measured precisely using remote sensing products. However, both air temperature and soil moisture can be difficult to detect using remote sensing platforms, especially in forests. While there have been advancements in remote sensing of soil moisture in recent decades (Babaeian et al., 2019), this information could still prove difficult to obtain at spatial and temporal scales that are compatible with the other remote sensing information used in these models. Air temperature may also need to be derived from a nearby weather station for a practical application of some of these models, which may also pose scaling problems. Thus, to use some of the models presented in this study, meteorological reanalysis data may be needed. However, despite these challenges the results of this project show promise for using remotely sensed $T_L$ as a proxy for intra-annual SRVs in subalpine forests of the Intermountain West.

Chapters 2 and 3 both showed intriguing linkages between remote sensing information and stem radial growth. However, both studies highlight the importance of scaling in remote sensing studies and show that more work needs to be done to accurately scale SRV measurements acquired with point dendrometers to a level that is ecologically relevant for most spaceborne remote sensing data. In Chapter 2, the large size (500 m) of MODIS pixels and the heterogeneity of the landscape within these pixels appeared to affect SDD estimates, causing them to be earlier than in-situ SDD estimates. Chapter 3 results show that branch level $T_L$ can predict intra-annual SRVs, but more research is needed to determine if these relationships are scalable to the canopy, and landscape levels. This scaling issue is common in remote sensing studies and there is a wealth of information available to address this (Kerr and Ostrovsky, 2003; Marceau and Hay, 1999). However, little of this work has focused on scaling intra-annual stem radial growth measured with point dendrometers to relevant scales. There are some important considerations when scaling stem radial growth, including stem density in the area of interest, the number and types of tree species, size of the trees, etc. All these factors will influence the scaling of stem radial growth to some degree, yet how is still relatively unknown. Thus, more research is clearly needed into scaling stem radial growth measurements to spatial scales relevant for spaceborne remote sensing products.

While there are still key challenges that need to be addressed, the results from

Chapters 2 and 3 demonstrate that there is promise for using remote sensing measurements to track stem radial growth in temperate and boreal forests of North America. While combining these sources of data is a relatively new area of research, these approaches are urgently needed given the linkages between stem radial growth and global water and C cycles. The studies presented here did not provide new methods for monitoring stem radial growth using remote sensing information; however, they do provide a critical first step in developing these new, robust approaches for monitoring stem radial growth in the forests of North America using satellite remote sensing approaches.

***References***

Babaeian, E., Sadeghi, M., Jones, S.B., 2019. Ground, Proximal, and Satellite Remote Sensing of Soil Moisture. Rev. Geophys. 57, 530–616. https://doi.org/10.1029/2018RG000618

Ensminger, I., Sveshnikov, D., Campbell, D.A., Funks, C., Jansson, S., Lloyd, J., Shibistova, O., Oquist, G., 2004. Intermittent low temperatures constrain spring recovery of photosynthesis in boreal Scots pine forests. Glob. Chang. Biol. 10, 995–1008. https://doi.org/10.1111/j.1365-2486.2004.00781.x

Fisher, J.B., Lee, B., Purdy, A.J., Halverson, G.H., Dohlen, M.B., Nicholson, K.C., Wang, A., Anderson, R.G., Aragon, B., Arain, M.A., Baldocchi, D.D., Baker, J.M., Barral, H., 2020. ECOSTRESS : NASA ' s Next Generation Mission to Measure Evapotranspiration From the International Space Station Water Resources Research. Water Resour. Res. 56, 1–20. https://doi.org/10.1029/2019WR026058

Kerr, J.T., Ostrovsky, M., 2003. From space to species: Ecological applications for remote sensing. Trends Ecol. Evol. 18, 299–305. https://doi.org/10.1016/S0169-5347(03)00071-5

Kirdyanov, A., Hughes, M., Vaganov, E., Schweingruber, F., Silkin, P., 2003. The importance of early summer temperature and date of snow melt for tree growth in the Siberian Subarctic. Trees 17, 61–69. https://doi.org/10.1007/s00468-002-0209-z

Marceau, D.J., Hay, G.J., 1999. Remote sensing contributions to the scale issue. Can. J. Remote Sens. 25, 357–366. https://doi.org/10.1080/07038992.1999.10874735

Parazoo, N.C., Arneth, A., Pugh, T.A.M., Smith, B., Steiner, N., Luus, K., Commane, R., Benmergui, J., Stofferahn, E., Liu, J., Rödenbeck, C., Kawa, R., Euskirchen, E., Zona, D., Arndt, K., Oechel, W., Miller, C., 2018. Spring photosynthetic onset and net CO2 uptake in Alaska triggered by landscape thawing. Glob. Chang. Biol. 24, 3416–3435. https://doi.org/10.1111/gcb.14283

Raleigh, M.S., Rittger, K., Moore, C.E., Henn, B., Lutz, J.A., Lundquist, J.D., 2013. Ground-based testing of MODIS fractional snow cover in subalpine meadows and forests of the Sierra Nevada. Remote Sens. Environ. 128, 44–57. https://doi.org/10.1016/j.rse.2012.09.016

Reinmann, A.B., Susser, J.R., Demaria, E.M.C., Templer, P.H., 2018. Declines in northern forest tree growth following snowpack decline and soil freezing. Glob. Chang. Biol. 420–430. https://doi.org/10.1111/gcb.14420

Reinmann, A.B., Templer, P.H., 2016. Reduced Winter Snowpack and Greater Soil Frost Reduce Live Root Biomass and Stimulate Radial Growth and Stem Respiration of Red Maple (Acer rubrum) Trees in a Mixed-Hardwood Forest. Ecosystems 19, 129–141. https://doi.org/10.1007/s10021-015-9923-4

Rossi, S., Morin, H., Deslauriers, A., 2011. Multi-scale influence of snowmelt on xylogenesis of black spruce. Arctic, Antarct. Alp. Res. 43, 457–464.

Tanja, S., Berninger, F., Vesala, T., Markkanen, T., Hari, P., Mäkelä, A., Ilvesniemi, H., Hänninen, H., Nikinmaa, E., Huttula, T., Laurila, T., Aurela, M., Grelle, A., Lindroth, A., Arneth, A., Shibistova, O., Lloyd, J., 2003. Air temperature triggers the recovery of evergreen boreal forest photosynthesis in spring. Glob. Chang. Biol. 9, 1410–1426.

Vaganov, E.A., Hughes, M.K., Kirdyanov, A. V, Schweingruber, F.H., Silkin, P.P., 1999. Influence of snowfall and melt timing on tree growth in subarctic Eurasia. Nature 400, 149–151.